



## OPEN ACCESS

## EDITED BY

Hartmut Jaeschke,  
University of Kansas Medical Center Research  
Institute, United States

## REVIEWED BY

Wei Zhong,  
University of Kansas Medical Center,  
United States  
Wei Guo,  
University of North Carolina at Greensboro,  
United States

## \*CORRESPONDENCE

Shou-Dong Guo,  
✉ sd-guo@sdsu.edu.cn

<sup>†</sup>These authors have contributed equally to  
this work

RECEIVED 19 November 2024

ACCEPTED 08 January 2025

PUBLISHED 03 February 2025

## CITATION

Zhang X-Y, Lu Q-Q, Li Y-J, Shi S-R, Ma C-N,  
Miao M and Guo S-D (2025) Conditional  
knockdown of hepatic PCSK9 ameliorates high-  
fat diet-induced liver inflammation in mice.  
*Front. Pharmacol.* 16:1528250.  
doi: 10.3389/fphar.2025.1528250

## COPYRIGHT

© 2025 Zhang, Lu, Li, Shi, Ma, Miao and Guo.  
This is an open-access article distributed under  
the terms of the [Creative Commons Attribution  
License \(CC BY\)](https://creativecommons.org/licenses/by/4.0/). The use, distribution or  
reproduction in other forums is permitted,  
provided the original author(s) and the  
copyright owner(s) are credited and that the  
original publication in this journal is cited, in  
accordance with accepted academic practice.  
No use, distribution or reproduction is  
permitted which does not comply with these  
terms.

# Conditional knockdown of hepatic PCSK9 ameliorates high-fat diet-induced liver inflammation in mice

Xue-Ying Zhang<sup>†</sup>, Qing-Qing Lu<sup>†</sup>, Yan-Jie Li<sup>†</sup>, Shan-Rui Shi,  
Chao-Nan Ma, Miao Miao and Shou-Dong Guo<sup>\*</sup>

Institute of Lipid Metabolism and Atherosclerosis, School of Pharmacy, Shandong Second Medical University, Weifang, China

**Instruction:** Accumulating evidence has shown that proprotein convertase subtilisin/kexin type 9 (PCSK9) is associated with inflammation in the vascular system. However, the roles of PCSK9 in hepatic inflammation remain unclear. Because PCSK9 is mainly expressed in the liver and modulates lipid uptake through low-density lipoprotein receptor family members, the present study aimed to elucidate the effect of conditional knockdown of hepatic PCSK9 on hyperlipidemia-induced inflammation and the underlying mechanisms of action.

**Methods:** PCSK9<sup>flox/flox</sup> mice were bred with ALB-Cre<sup>+</sup> mice to obtain hepatic PCSK9<sup>(-/-)</sup>, PCSK9<sup>(+/-)</sup>, and PCSK9<sup>(+/+)</sup> mice. These mice were fed with a high-fat diet for 9 weeks to induce inflammation. The effects of conditional knockdown of hepatic PCSK9 on inflammation and the underlying mechanisms were investigated by molecular biological techniques. Moreover, the findings were verified in vitro using HepG2 cells.

**Results and Discussion:** Conditional knockdown of hepatic PCSK9 remarkably decreased plasma levels of total cholesterol and alleviated hyperlipidemia-induced liver injury. Mechanistically, conditional knockdown of hepatic PCSK9 significantly reduced the levels of pro-inflammatory factors by downregulating the expression of Toll-like receptors, mitogen-activated protein kinase (MAPK), and phosphoinositide-3 kinase/protein kinase B, which subsequently attenuated the expression of downstream molecules, namely nuclear factor kappa-B and activator protein-1. The related mechanisms were confirmed using lipid-loaded HepG2 cells together with PCSK9 siRNA, alirocumab (anti-PCSK9 antibody), and/or a p38-MAPK inhibitor. These findings confirmed that conditional knockdown of hepatic PCSK9 attenuates liver inflammation following hyperlipidemia induction by modulating multiple signaling pathways; this suggests that

**Abbreviations:** AKT, protein kinase B; ALT, alanine aminotransferase; AP-1, activator protein-1; AST, aspartate aminotransferase; CVD, cardiovascular disease; CD36, cluster of differentiation 36; DMEM, Dulbecco's modified Eagle's medium; ERK1/2, extracellular regulated protein kinase 1/2; FPLC, fast protein liquid chromatography; GAPDH, glyceraldehyde-3-phosphate dehydrogenase; HDL, high-density lipoprotein; IL, interleukin; JAK, janus kinase; JNK, c-Jun N-terminal kinase; LDLR, low-density lipoprotein receptor; LPS, lipopolysaccharide; MAFLD, metabolic dysfunction-associated fatty liver disease; MAPK, mitogen-activated protein kinase; mTOR, mammalian target of rapamycin; MyD88, myeloid differentiation factor 88; MASH, metabolic dysfunction-associated steatohepatitis; NF-κB, nuclear factor kappa-B; PCSK9, proprotein convertase subtilisin/kexin type 9; PI3K, phosphoinositide-3 kinase; PVDF, Polyvinylidene fluoride; TBS, Tris-buffered saline; TC, total cholesterol; TG, triglycerides; TLR, toll-like receptor; TNF, tumor necrosis factor.

targeting PCSK9 knockdown/inhibition with appropriate agents is useful not only for treating hyperlipidemia but also for ameliorating hyperlipidemia-induced liver inflammation.

#### KEYWORDS

inflammation, MAPK, PCSK9 inhibitor, PCSK9 siRNA, Toll-like receptor

## Introduction

Loss-of-function mutations in the hepatic protein proprotein convertase subtilisin/kexin type 9 (PCSK9) reduce plasma low-density lipoprotein (LDL) cholesterol (LDL-c) levels, and vice versa (Meng et al., 2023). Mechanistically, PCSK9 interacts with LDL receptor (LDLR) and other LDLR family members to induce their degradation, leading to development of hyperlipidemia. Compared to statins, PCSK9 inhibitors, such as monoclonal antibodies evolocumab and alirocumab, exhibit more robust effects in reducing LDL-c levels (Zhang et al., 2007; Dixon et al., 2016; Coppinger et al., 2022; Momtazi-Borojeni et al., 2022). Therefore, together with statin therapy, anti-PCSK9 antibodies are currently used for the clinical treatment of hyperlipidemia to decrease the risk of residual cardiovascular diseases (CVDs), a leading cause of death in humans. With advancement in research on PCSK9, this hepatic protein was shown to possess multifaceted functions; furthermore, PCSK9 inhibitors were found to exhibit LDL-c-independent effects (Ferri and Ruscica, 2016; Ugovšek and Šebešljen, 2022). Moreover, given that atherosclerosis, the basic pathological change occurring in CVD, is primarily promoted by chronic inflammation induced by hyperlipidemia (Zhao et al., 2021), the role of PCSK9 in inflammation has attracted the attention of many researchers in recent years.

In African Americans with CVD, the fasting levels of inflammatory cytokine interleukin (IL)-8 is positively associated with PCSK9 (Baginski et al., 2022). In a rat model, hepatic PCSK9 synthesis level and circulating PCSK9 level are related to plasma IL-13 levels (Low et al., 2020). Moreover, plasma PCSK9 levels show a positive association with the levels of proinflammatory factors, including IL-6, IL-1 $\beta$ , and tumor necrosis factor (TNF)- $\alpha$  (Ding et al., 2020a; Punch et al., 2022). Based on these observations, PCSK9 and inflammation appear to have a mutual promoting effect. On the one hand, inflammatory stimuli increase PCSK9 secretion in macrophages and some tissues, including aorta and heart (Andreadou et al., 2020). For example, TNF- $\alpha$  and interferon  $\gamma$  synergistically promote PCSK9 expression by upregulating sterol regulatory element binding protein 2 *in vitro* (Zhang et al., 2023). In addition to proinflammatory cytokines, high-fat diet (HFD)-induced hyperlipidemia also enhances PCSK9 expression potentially by modulating Toll-like receptor (TLR) 4 and its downstream signaling factors myeloid differentiation primary response gene 88 (MyD88) and nuclear factor kappa-B (NF- $\kappa$ B) (Liu et al., 2020). On the other hand, PCSK9 can also induce inflammation by elevating lipid accumulation in macrophages and enhancing the TLR/NF- $\kappa$ B signaling pathway (Andreadou et al., 2020); this process is mediated by LDLR-related protein 5 (Badimon et al., 2021). Consistent with this observation, adeno-associated virus-mediated

overexpression of PCSK9 promotes atherosclerosis development and increases the numbers of proinflammatory monocytes/macrophages in C57BL/6J mice (Peled et al., 2017; Keeter et al., 2022). Furthermore, lentivirus carrying PCSK9 small hairpin RNA attenuates aortic inflammation by suppressing the TLR-4/NF- $\kappa$ B signaling pathway (Tang et al., 2017; Yurtseven et al., 2020). These findings indicate that PCSK9 is closely associated with vascular inflammation.

HFD-induced hyperlipidemia is a known high-risk factor for the development of nonalcoholic steatohepatitis and nonalcoholic fatty liver disease; the former has been recently renamed as metabolic dysfunction-associated steatohepatitis (MASH) and the latter has been recently renamed as metabolic dysfunction-associated fatty liver disease (MAFLD) (Lebeau et al., 2019; Wu et al., 2023; Fang et al., 2024). Although PCSK9 shows a positive relationship with body mass index and is considered to be associated with metabolic syndrome (Ferri and Ruscica, 2016), the effects of PCSK9 on MASH and MAFLD are contradictory (Momtazi-Borojeni et al., 2022). Importantly, the role of PCSK9 in hepatic inflammation and the underlying mechanisms of action have been seldomly reported because previous studies mainly focused on hepatic PCSK9-mediated lipid metabolism. Notably, PCSK9-deficiency was shown to increase liver weight, hepatic TG accumulation, and inflammation in mice by upregulating CD36-mediated fatty acid internalization and TG storage (Demers et al., 2015). This was particularly observed in PCSK9-deficient mice fed an HFD (Lebeau et al., 2019), thus suggesting that the complete deletion of PCSK9 induces MAFLD and MASH (Lebeau et al., 2022). However, because PCSK9 deficiency is an extreme condition, the related studies with PCSK9-deficient models may have inaccurately predicted the role of PCSK9 in hyperlipidemia-induced inflammation. Because the secretory PCSK9 protein is also produced by the intestine and other tissues (Zaid et al., 2008), we hypothesized that conditional knockdown of hepatic PCSK9 could attenuate hyperlipidemia-induced liver inflammation as PCSK9 secreted by extrahepatic tissues is transported to the liver, thereby partially compensating PCSK9 deficiency. The present study aimed to validate this hypothesis by using PCSK9<sup>liver(-/-)</sup>, PCSK9<sup>liver(+/-)</sup>, and PCSK9<sup>liver(+/+)</sup> mice.

## Materials and methods

### Materials

Isoflurane (R510-22-10) was bought from RWD Life science Co., Ltd. (Shenzhen, China). Adezmapimod (SB203580), a potent p38-MAPK inhibitor, was purchased from Selleck chemicals, LLC, United States. An anti-PCSK9 monoclonal antibody, alirocumab, was obtained from Sanofi S.A. Penicillin-streptomycin liquid

TABLE 1 The primers for identification of ALB and PCSK9.

Primers	Sequence (5'-3')	Molecular weight
ALB primer 1-Forward 1	GGGCAGTCTGGTACTTCCAAGCT	Target: 340 bp
ALB primer 1-Reverse 1	TAGTACCTATGCGATCCAAACAAC	Wild type: None
ALB primer 2- Forward 2	CCTGCTGTCCATTCTTATTCAT	Target: 356 bp
ALB primer 2-Reverse 2	ATATCCCCTTGTTCCTTCTGTC	Wild type: None
ALB primer 3-Forward 3	CAGCAAAACCTGGCTGTGGATC	Target: None
ALB primer 3-Reverse 3	ATGAGCCACCATGTGGGTGTC	Wild type: 412 bp
PCSK9 primer 1- Forward 1	TGGCAGTCAGGAGCAGTATGTCCAT	Target: 378 bp
PCSK9 primer 1-Reverse 1	GAATCTTGAGTTGCACCAATCATTGG	Wild type: 278 bp
PCSK9 primer 2- Forward 2	CTAAACCCGACTGACCCACTATTTG	Target: 346 bp
PCSK9 primer 2-Reverse 2	CAGTCCTACCAGATCCAGACCACCTT	Wild type: 245bp

(P1400), 0.25% trypsin-EDTA solution (T1300), palmitic acid (N-16-A), and cis-9-octadecenoic acid (IC1350) were purchased from Solarbio Life Sciences (Beijing, China). Human hepatocellular carcinoma cell line HepG2 (SCSP-150) was bought from the Cell Bank of Chinese Academy of Sciences (Shanghai, China). Lipofectamine 3,000 reagent (L3000008) was purchased from Invitrogen Corporation, United States. Dulbecco's modified Eagle's medium (DMEM) (C11995500BT) and Opti-MEM I reduced serum medium (31,985,062) were the products of Gibco ThermoFisher Scientific Corporation (CA, United States). Fetal bovine serum (FBS) (BS1612-105) was obtained from Bioexplorer Life Sciences (C.A., China). High-fat diet (License No.: SCXK 2020-0004) was the product of Keao Xieli Feed Co., Ltd. (Tianjin, China). Heparinized capillary tubes (2501) were purchased from Kimble Chase Life Science and Research Products LLC. (NJ, United States). NEG-50™ frozen section medium (6502) was bought from Richard-Allan Scientific LLC. (Kalamazoo, MI, United States). The assay kits for total cholesterol (TC, 100,000,180) and TG (100,000,220) were provided by Biosino Bio-technology and Science Inc. (Beijing, China). The antibody information was provided in [Supplementary Table S1](#). The rest reagents used in this study were of analytical grade.

### Mouse breeding

Animal experiments were approved by the Laboratory Animal Ethical Committee of Shandong Second Medical University and carried out according to NIH guidelines for the Care and Use of Animals (2020SDL106). In this study, PCSK9<sup>fllox/flox</sup> mice and albumin (Alb)-Cre mice were purchased from GemPharmatech LLC. (Jiangsu, China). The mice were kept in a temperature-controlled room (23°C) with controlled light/dark cycles (12 h/12 h). PCSK9<sup>fllox/flox</sup> mice were bred with Alb-Cre mice to produce Alb-Cre<sup>+</sup>/PCSK9<sup>fllox/flox</sup> (PCSK9<sup>liver(+/+)</sup> or wild type) mice, Alb-Cre<sup>+</sup>/PCSK9<sup>fllox/flox</sup> (hepatic-specific PCSK9 knockout, PCSK9<sup>liver(-/-)</sup>) mice; and Alb-Cre<sup>+</sup>/PCSK9<sup>fllox/WT</sup> (PCSK9<sup>liver(+/-)</sup>) mice. The primers for genotyping are listed in [Table 1](#).

### Animal grouping and intervention with a high-fat diet

Approximately 10-week-old male PCSK9<sup>liver(+/+)</sup> (n = 10), PCSK9<sup>liver(-/-)</sup> (n = 10), and PCSK9<sup>liver(+/-)</sup> (n = 6) mice were fed an HFD containing 21% fat and 0.15% cholesterol for 9 weeks. On the last day of HFD feeding, mice were fasted for 6 h, weighted, and anaesthetized using isoflurane before sampling. Briefly, mouse blood was collected from the retro-orbital venous plexus by using heparinized capillary tubes, and plasma was obtained by centrifugation of the blood samples at 1,100 × g for 30 min. Next, mouse heart was exposed, and the auricle was cut using surgical scissors. The mouse was perfused with phosphate buffer saline (PBS, pH = 7.4) through the left ventricle to remove the residual blood before sampling. For comparative analyses, 6 age-matched PCSK9<sup>fllox/flox</sup> mice fed a chow diet were randomly selected for plasma levels of TC and TG determination and Western blotting experiments.

### Plasma and liver analysis

Plasma TC and TG levels were determined using appropriate assay kits in accordance with the manufacturers' instructions. To determine TC and TG distributions in very low-density lipoprotein (VLDL), LDL, and high-density lipoprotein (HDL) particles, mixed plasma (100 μL) from each group was analyzed using a Superose™ 6 10/300 gel chromatography column linked to an ÄKTA Fast Protein Liquid Chromatography (FPLC) system. The column was eluted with 0.9% sodium chloride solution, and the eluate was collected using an automatic collector with 0.5 mL in each fraction. Hepatic lipids were extracted as reported previously with minor modifications ([Tran et al., 2020; Li et al., 2022](#)). Briefly, approximately 100 mg liver samples were homogenized in 1 mL PBS, and 4 mL chloroform and methanol mixture (2:1, v/v) was added and shaken well. This suspension was centrifuged at 1800 × g for 10 min to obtain the bottom chloroform phase containing lipid, which was subjected to blow-drying with nitrogen. The obtained lipids were resolved in 100 μL ethanol and used for determining TC and TG levels by using commercially available assay kits as described above.

TABLE 2 The primers used for polymerase chain reaction (PCR).

Name	Primers	Sequence (5'-3')
<i>h</i> -PCSK9	Forward	GGCAGAGACUGAUCCACUUtTdT
	Reverse	dTdTCCGUCUCUGACUAGGUGAA
<i>siRNA1</i>	Forward	GGGUCAUGGUCACCGACUUt
	Reverse	AAGUCGGUGACCAUGACCCtg
<i>m</i> -GAPDH	Forward	AAGAAGGTGGTGAAGCAGGCATC
	Reverse	CGGCATCGAAGGTGGAAGAGTG
<i>m</i> -PCSK9	Forward	AGGCACAGGCTGA TCCACTTCT
	Reverse	AGCAGCCCAACAACCTCTCATC
<i>m</i> -LDLR	Forward	GCAGCCACATGGTATGAGGTTC
	Reverse	TGATGTTCTTCAGCCGCCAGTTC
<i>m</i> -P65	Forward	CTCCTGTTTCATCCGACTCCC
	Reverse	AGTCAGTGCCTGTTTACGTT
<i>m</i> -P38	Forward	GGCAGGAGCTGAACAAGACCATC
	Reverse	AGCAGACGCAACTCTCGGTAGG
<i>m</i> -ERK1/2	Forward	GCCTTCCAACCTCCTGCTGAAC
	Reverse	CGTACTCTGTCAAGAACCCTGTGTG
<i>m</i> -JNK	Forward	CGCCTTATGTGGTGACTCGCTAC
	Reverse	CTCCCATGATGCACCAACTGAC
<i>m</i> -TLR2	Forward	AAGATGCGCTTCCTGAATTTG
	Reverse	TCCAGCGTCTGAGGAATGC
<i>m</i> -TLR4	Forward	ATGGCATGGCTTACACCACC
	Reverse	GAGGCCAATTTTGTCTCCACA
<i>m</i> -PI3K	Forward	TGCAGCACAATGACTCCC
	Reverse	TTCATCGCCTCTGTTGTGCAT
<i>m</i> -AKT	Forward	TTCACAACCAGGACCAGCAGA
	Reverse	ATCCATGAGGATCAGCTCGAAC
<i>m</i> -mTOR	Forward	ACCGTCCGCCTTCACAGATAC
	Reverse	CGTTCCTTCTCCTTCTTGACACAG
<i>m</i> -IL-6	Forward	CTTCTTGGGACTGATGCTGGTGAC
	Reverse	TCTGTTGGGAGTGGTATCCTCTGTG
<i>m</i> -IL-1β	Forward	CCAGGATGAGGACATGAGCA
	Reverse	CGGAGCCTGTAGTGCAGTTG
<i>m</i> -TNFα	Forward	ACTCCAGGCGGTGCCTATGT
	Reverse	AGTGTGAGGGTCTGGGCCAT

Haematoxylin and eosin (H & E) staining and Oil Red O staining

Liver tissues were fixed with freshly prepared 4% paraformaldehyde for 24 h, embedded in paraffin by using a JB-

P5 embedding machine (Wuhan, China), and cut into 7-μm-thick sections by using a RM2016 pathology slicer (Shanghai, China). Next, the sections were dewaxed in xylene, passed through a gradient of ethanol concentrations, and rinsed with tap water. Subsequently, the sections were stained with hematoxylin solution for 4 min, rinsed with tap water, and stained with eosin for 15 s. Finally, the sections were dehydrated and sealed with neutral gum (Zhang et al., 2022). For Oil Red O staining, fresh liver tissues were dissected, dried with a filter paper, trimmed into a cube shape (side length: 5 mm), and embedded in NEG-50™ frozen section medium. Next, the tissues were fixed on the slicer, and 8-μm-thick tissue sections were obtained using a Cryostar NX50 machine (Thermo, United States). The sections were subsequently stained with freshly prepared Oil Red O dye solution (Yin et al., 2019). The stained images were recorded on an Axiocam 506 color camera (Zeiss, Jena, Germany), and the staining areas were analyzed by using ImageJ software.

Lipid accumulation induced inflammation in HepG2 cells

HepG2 cells were seeded in 6-well plates at a density of  $2.0 \times 10^5$ /well. The cells were cultured in a humidified 5% CO<sub>2</sub> at 37°C. These cells were randomly divided into blank, model, alirocumab (Pm, 10 μg/mL), SB203580 (p38i, 30 μM), and combination (Pm + i, alirocumab 10 μg/mL and SB203580 30 μM) groups. Except for the blank group, the rest groups were treated with 0.5 mM cis-9-octadecenoic acid and 0.25 mM palmitic acid for 24 h to establish a lipid-loaded cell model (Li et al., 2020; Zulkapli et al., 2023; Zhang et al., 2024). Next, the cells were treated with the corresponding drugs for another 24 h prior to sampling.

For the siRNA transfection experiments, the HepG2 cells were initially incubated with 0.5 mM cis-9-octadecenoic acid and 0.25 mM palmitic acid for 24 h to establish a lipid-loaded cell model. Next, the cells were randomly divided into negative control (NC), PCSK9 siRNA1 (siR-1), and PCSK9 siRNA2 (siR-2) groups. The siRNAs against PCSK9 were synthesized by Guangzhou RiboBio Co., Ltd. (Guangzhou, China) and the sequences were listed in Table 2 (Tang et al., 2012; Xiao et al., 2019). Briefly, the cells were transfected with the corresponding siRNA by using Lipofectamine 3,000 as reported previously (Tang et al., 2012; Deng et al., 2020). The cells were cultivated for another 24 h prior to sampling. In this study, the normal HepG2 cells were used as blank control. Moreover, the expression levels of several inflammation-related proteins in the blank control, model, and NC groups were investigated to confirm lipid accumulation-induced inflammation and to rule out the potential effects caused by the control plasmid.

Immunoblotting

Approximately 50 mg liver tissues were homogenized in 500 μL RIPA lysis buffer and allowed to digest on ice for 30 min. The protein concentration was adjusted to approximately 3.0 g/mL according to the results of the bicinchoninic acid assay. The cell sample in each well was treated with 60 μL RIPA lysis buffer to



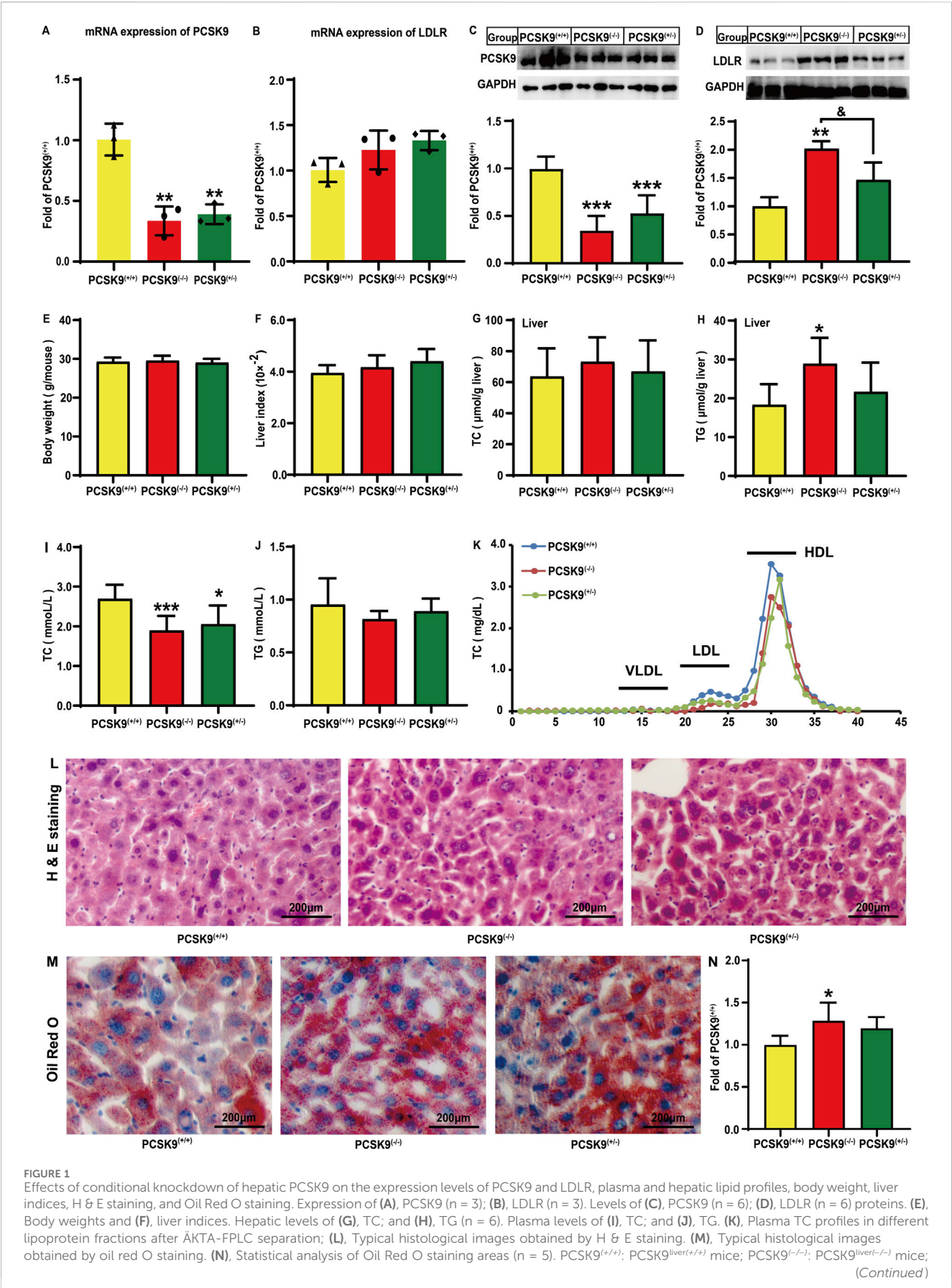


**FIGURE 1** Effects of conditional knockdown of hepatic PCSK9 on the expression levels of PCSK9 and LDLR, plasma and hepatic lipid profiles, body weight, liver indices, H & E staining, and Oil Red O staining. Expression of (A), PCSK9 (n = 3); (B), LDLR (n = 3). Levels of (C), PCSK9 (n = 6); (D), LDLR (n = 6) proteins. (E), Body weights and (F), liver indices. Hepatic levels of (G), TC; and (H), TG (n = 6). Plasma levels of (I), TC; and (J), TG. (K), Plasma TC profiles in different lipoprotein fractions after ÄKTA-FPLC separation; (L), Typical histological images obtained by H & E staining. (M), Typical histological images obtained by oil red O staining. (N), Statistical analysis of Oil Red O staining areas (n = 5). PCSK9<sup>+/+</sup>; PCSK9<sup>liver(-/-)</sup> mice; PCSK9<sup>-/-</sup>; PCSK9<sup>liver(-/-)</sup> mice; (Continued)

## FIGURE 1 (Continued)

PCSK9<sup>liver(+/-)</sup>; PCSK9<sup>liver(-/-)</sup> mice. For (E, F, I, J), PCSK9<sup>liver(+/+)</sup> (n = 10), PCSK9<sup>liver(-/-)</sup> (n = 10), PCSK9<sup>liver(+/-)</sup> (n = 6). These abbreviations are suitable for the rest figures. \*means  $p < 0.05$  vs. PCSK9<sup>liver(+/+)</sup> group; \*\*means  $p < 0.01$  vs. PCSK9<sup>liver(+/+)</sup> group; \*\*\*means  $p < 0.001$  vs. PCSK9<sup>liver(+/+)</sup> group; <sup>b</sup>means  $p < 0.05$  vs. PCSK9<sup>liver(+/-)</sup> group.

obtain total proteins. This experiment was conducted by following previously reported methods (Li et al., 2020; Fu et al., 2021; Zhang et al., 2022; Zulkapli et al., 2023; Zhang et al., 2024). In brief, equal amounts of proteins were separated by sodium dodecyl sulfate-polyacrylamide gel electrophoresis on gels with different concentrations (6%–12%). The separated proteins were transferred onto 0.45  $\mu$ m polyvinylidene fluoride (PVDF) membranes (or 0.22  $\mu$ m PVDF membranes for proteins with a molecular weight of <30 kDa) by electroblotting. These PVDF membranes were blocked with 5% nonfat dry milk dissolved in Tris-buffered saline (TBS) at room temperature for 2–4 h. Next, these PVDF membranes were incubated with the corresponding primary antibodies at 4°C for 12 h. The PVDF membranes were then washed with TBS containing 0.1% Tween for 3–5 times and incubated with the corresponding secondary antibodies for 2 h at room temperature. Finally, immunoblots were visualized by enhanced chemiluminescence reaction, and the images were captured with an SH-Compact 523 ECL imaging system, a product of Shenhua Science Technology Co., Ltd. (Hangzhou, China). Densitometry analysis was conducted using ImageJ software. The protein levels were normalized by housekeeping protein glyceraldehyde-3-phosphate dehydrogenase (GAPDH) or  $\beta$ -actin.

## Quantitative reverse transcription-polymerase chain reaction (RT-qPCR)

An appropriate amount of liver tissue (~50 mg) was ground to powder under liquid nitrogen protection in a RNase free mortar. The obtained powder was extracted with Trizol (Spark Jade, Qingdao, China) in accordance with the manufacturer's instructions. The concentration and purity of total RNA were determined by estimating the absorbance at 260 nm and 280 nm with a NanoDrop™ OneC UV spectrophotometer (Thermo Fisher, United States). cDNA was subsequently synthesized in an ABI Veriti™ 96-well thermal cycler (MA, United States) in accordance with the manufacturer's instructions. RT-qPCR was performed in an ABI QuantStudio3 PCR system (Waltham, MA, United States) as reported previously (Yang et al., 2019; Li et al., 2020; Li et al., 2022). Gene-specific primers (Table 2) were designed and synthesized by Sangon Biotechnology Co., Ltd. (Shanghai, China). The relative expression of target genes was adjusted based on the  $C_t$  number of GAPDH and calculated according to the  $2^{-\Delta\Delta C_t}$  method.

## Data analysis

Statistical analysis was performed using one-way analysis of variance (ANOVA). The results were presented as the mean  $\pm$

standard deviation (SD) for at least three independent experiments. Calculations were performed using GraphPad Prism software, version 7.0 (San Diego, CA, United States). Differences were considered to be significant at a  $P < 0.05$ .

## Results

### Generation of hepatic PCSK9 conditional knockdown mice

After several rounds of breeding, we obtained colonies of hepatic PCSK9<sup>liver(+/+)</sup>, PCSK9<sup>liver(+/-)</sup>, and PCSK9<sup>liver(-/-)</sup> mice based on the genotyping results (Supplementary Figure S1). We used three and two pairs of primers to determine the gene phenotype of ALB-Cre<sup>+</sup> and PCSK9<sup>flox/flox</sup>, respectively. Table 1 shows the primers and target molecular weight for identifying PCSK9<sup>liver(+/+)</sup>, PCSK9<sup>liver(+/-)</sup>, and PCSK9<sup>liver(-/-)</sup> mice. Taking the mice numbered as 1–9 for example: mice number 3, 4, and 6–9 were determined as PCSK9<sup>liver(-/-)</sup> mice, while mice number 1, 2, and 5 were determined as PCSK9<sup>liver(+/-)</sup> mice according to the molecular weight of the observed bands following agarose gel electrophoresis (Supplementary Figures S1A–C). In summary, hepatic PCSK9 conditional knockdown mice were successfully bred in our laboratory. Next, we investigated whether hepatic PCSK9 knockdown ameliorates hyperlipidemia-induced inflammation. The *in vivo* experimental design was shown in Supplementary Figure S1D.

### Effects of conditional knockdown of hepatic PCSK9 on PCSK9 and LDLR expression levels, lipid profile, and liver injury following HFD challenge

First of all, we demonstrated that HFD successfully induced hyperlipidemia in mice compared to those fed a chow diet (Figures 1I, J, Supplementary Figures S2A, B). Importantly, the levels of PCSK9, TNF- $\alpha$ , IL-1 $\beta$ , TLR-2, and TLR-4, and the levels of phosphorylated NF- $\kappa$ B, AP-1, MyD88, phosphoinositide 3-kinase (PI3K), protein kinase B (PKB/AKT), mTOR, p38-MAPK, and ERK1/2 proteins were significantly upregulated in the liver of PCSK9<sup>liver(+/+)</sup> mice fed a high-fat diet, as compared to the mice fed a chow diet (Supplementary Figure S2 and Supplementary Material S1). These results revealed the hyperlipidemia induces inflammation in liver by affecting multiple signaling pathways. In the following sections, we aimed to determine the effects of conditional knockdown of hepatic PCSK9 and the underlying mechanisms of action on modulating hyperlipidemia-induced chronic liver inflammation.

The gene and protein expression levels of hepatic PCSK9 and LDLR were determined in mice fed an HFD. As expected, compared

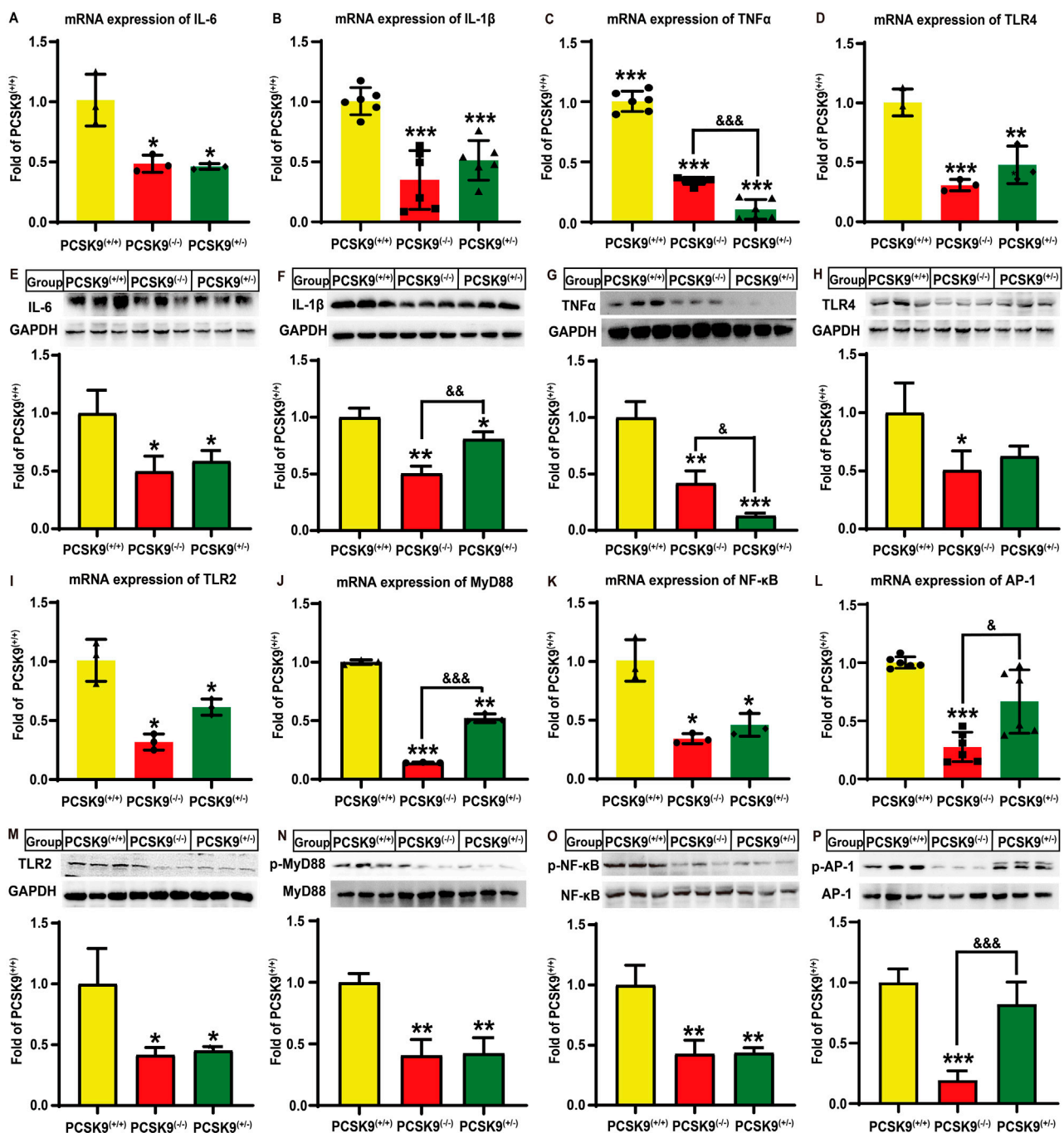


**FIGURE 2**  
Effects of conditional knockdown of hepatic PCSK9 on some hepatic inflammation-related molecules in mice fed an HFD. Expression of (A), IL-6 (n = 3); (B), IL-1β (n = 6); (C), TNFα (n = 6); and (D), TLR4 (n = 3). Levels of (E), IL-6; (F), IL-1β; (G), TNFα; and (H), TLR4 proteins (n = 6). Expression of (I), TLR2 (n = 3); (J), MyD88 (n = 3); (K), NF-κB (n = 3); and (L), AP-1 (n = 6) proteins. Levels of (M), TLR2; (N), phosphorylated MyD88; (O), phosphorylated p65-NF-κB; and (P), phosphorylated AP-1 proteins (n = 6). \*means  $p < 0.05$  vs. PCSK9<sup>liver(+/+)</sup> group; \*\*means  $p < 0.01$  vs. PCSK9<sup>liver(+/+)</sup> group; \*\*\*means  $p < 0.001$  vs. PCSK9<sup>liver(+/+)</sup> group; <sup>b</sup>means  $p < 0.05$  vs. PCSK9<sup>liver(+/-)</sup> group; <sup>b\*</sup>means  $p < 0.01$  vs. PCSK9<sup>liver(+/-)</sup> group; <sup>b\*\*</sup>means  $p < 0.001$  vs. PCSK9<sup>liver(+/-)</sup> group.

to PCSK9<sup>liver(+/+)</sup> mice, PCSK9<sup>liver(-/-)</sup> and PCSK9<sup>liver(+/-)</sup> mice exhibited a decrease in the mRNA expression level of PCSK9 by 66.4% and 60.9%, respectively ( $P < 0.01$ , Figure 1A). Conditional knockdown of hepatic PCSK9 did not affect the LDLR gene expression (Figure 1B). Consistent with this observation,

PCSK9<sup>liver(-/-)</sup> and PCSK9<sup>liver(+/-)</sup> mice showed a significant decrease in the hepatic PCSK9 levels by approximately 65.5% and 47.0%, respectively, as compared to PCSK9<sup>liver(+/+)</sup> mice ( $P < 0.05$ , Figure 1C). The hepatic LDLR levels were significantly increased by approximately 102% ( $P < 0.01$ ) and 46.7% in



PCSK9<sup>liver(-/-)</sup> and PCSK9<sup>liver(+/-)</sup> mice, respectively, as compared to those in PCSK9<sup>liver(+/+)</sup> mice (Figure 1D). Notably, PCSK9<sup>liver(-/-)</sup> mice exhibited significantly higher LDLR level than PCSK9<sup>liver(+/-)</sup> mice. As shown in Figures 1E, F, mice body weight and liver indices showed no significant changes (Supplementary Material S2). We also did not find alterations in hepatic TC levels among the mice groups (Figure 1G); however, the hepatic TG levels were increased by 57.8% in PCSK9<sup>liver(-/-)</sup> mice as compared to that in PCSK9<sup>liver(+/+)</sup> mice (Figure 1H). A noteworthy finding is PCSK9<sup>liver(-/-)</sup> and PCSK9<sup>liver(+/-)</sup> mice showed a decrease in plasma TC levels by 29.7% ( $P < 0.001$ ) and 23.4% ( $P < 0.05$ ), respectively, as compared to PCSK9<sup>liver(+/+)</sup> mice (Figure 1I). Consistent with this finding, ÅKTA-FPLC revealed a reduction in TC levels in LDL and HDL particles in hepatic PCSK9 knockdown mice, particularly in PCSK9<sup>liver(-/-)</sup> mice (Figure 1K and Supplementary Material S2). However, the groups showed no significant differences in plasma TG levels (Figure 1J). Additionally, H & E staining revealed no apparent alterations in the liver among the groups (Figure 1L and Supplementary Material S3). The Oil Red O staining areas increased by 28.6% and 19.7%, respectively, in the liver sections of the PCSK9<sup>liver(-/-)</sup> and PCSK9<sup>liver(+/-)</sup> mice as compared to those of the PCSK9<sup>liver(+/+)</sup> mice (Figures 1M, N, Supplementary Material S3). This finding was consistent with the higher levels of TG accumulation in the liver of hepatic PCSK9<sup>liver(-/-)</sup> mice as compared with those of PCSK9<sup>liver(+/+)</sup> mice (Figure 1H).

## Effects of conditional knockdown of hepatic PCSK9 on hyperlipidemia-induced liver inflammation and the TLR-2/4 signaling pathway

Next, we assessed whether hepatic PCSK9 affects hyperlipidemia-induced expression of proinflammatory cytokines in mice liver. Notably, conditional knockdown of hepatic PCSK9 remarkably decreased the mRNA expression levels of IL-6, IL-1 $\beta$ , and TNF $\alpha$  by 51.4% ( $P < 0.05$ ), 65.6% ( $P < 0.001$ ), and 66.1% ( $P < 0.001$ ), respectively, in PCSK9<sup>liver(-/-)</sup> mice as compared to those in PCSK9<sup>liver(+/+)</sup> mice (Figures 2A–C). Consistent with this finding, PCSK9<sup>liver(-/-)</sup> mice showed a decrease in IL-6, IL-1 $\beta$ , and TNF $\alpha$  protein levels by approximately 50.3% ( $P < 0.05$ ), 49.7% ( $P < 0.01$ ), and 58.3% ( $P < 0.01$ ), respectively, as compared to PCSK9<sup>liver(+/+)</sup> mice (Figures 2E–G). Moreover, IL-6, IL-1 $\beta$ , and TNF $\alpha$  expression levels were reduced by 54.4% ( $P < 0.05$ ), 49.3% ( $P < 0.001$ ), and 89.7% ( $P < 0.001$ ), respectively, in PCSK9<sup>liver(+/-)</sup> mice as compared to those in PCSK9<sup>liver(+/+)</sup> mice (Figures 2A–C). In line with these changes, PCSK9<sup>liver(+/-)</sup> mice exhibited a similar reduction in IL-6, IL-1 $\beta$ , and TNF $\alpha$  protein levels as compared to PCSK9<sup>liver(-/-)</sup> mice (Figures 2E–G). Notably, PCSK9<sup>liver(-/-)</sup> mice showed a further reduction in the IL-1 $\beta$  protein level as compared to PCSK9<sup>liver(+/-)</sup> mice ( $P < 0.01$ , Figure 2F). However, PCSK9<sup>liver(+/-)</sup> mice showed a significant reduction in TNF $\alpha$  mRNA ( $P < 0.001$ , Figure 2C) and protein expression levels ( $P < 0.05$ , Figure 2G) as compared to PCSK9<sup>liver(-/-)</sup> mice.

Given the important roles of TLR in inflammation, we investigated whether this signaling pathway was involved in the abovementioned process. Notably, hyperlipidemia stimulation significantly decreased the mRNA expression levels of TLR-4

(Figure 2D) and TLR-2 (Figure 2I) by 69.1% ( $P < 0.001$ ) and 68.1% ( $P < 0.05$ ), and 52.1% ( $P < 0.01$ ) and 38.6% ( $P < 0.05$ ), respectively, in PCSK9<sup>liver(-/-)</sup> and PCSK9<sup>liver(+/-)</sup> mice as compared to that of PCSK9<sup>liver(+/+)</sup> mice. Although both PCSK9<sup>liver(-/-)</sup> and PCSK9<sup>liver(+/-)</sup> mice groups exhibited a reduction in TLR-4 protein levels, only the former group showed a significant difference in the TLR-4 protein level as compared to the PCSK9<sup>liver(+/+)</sup> group ( $P < 0.05$ , Figure 2H). Conditional knockdown of hepatic PCSK9 also significantly reduced the TLR-2 protein level by approximately 58.3% and 54.8%, respectively, in both PCSK9<sup>liver(-/-)</sup> and PCSK9<sup>liver(+/-)</sup> mice groups ( $P < 0.05$ , Figure 2M). Moreover, PCSK9<sup>liver(-/-)</sup> and PCSK9<sup>liver(+/-)</sup> mice groups showed a reduction in MyD88 expression levels by 85.8% ( $P < 0.001$ ) and 47.8% ( $P < 0.01$ ), respectively, as compared to PCSK9<sup>liver(+/+)</sup> mice, with a significant difference between hepatic PCSK9<sup>liver(-/-)</sup> and PCSK9<sup>liver(+/-)</sup> mice groups ( $P < 0.001$ , Figure 2J). The phosphorylation levels of MyD88 were also decreased by approximately 59% in both PCSK9<sup>liver(-/-)</sup> and PCSK9<sup>liver(+/-)</sup> mice groups as compared to that in the PCSK9<sup>liver(+/+)</sup> group ( $P < 0.01$ , Figure 2N). Importantly, conditional knockdown of hepatic PCSK9 significantly reduced the gene expression ( $P < 0.05$ ) and phosphorylation levels of p65-NF- $\kappa$ B ( $P < 0.01$ ) as compared to that in PCSK9<sup>liver(+/+)</sup> mice (Figures 2K, O). Additionally, the AP-1 gene expression level was decreased by approximately 72.6% in PCSK9<sup>liver(-/-)</sup> mice, but not in PCSK9<sup>liver(+/-)</sup> mice, as compared to that in PCSK9<sup>liver(+/+)</sup> mice ( $P < 0.001$ , Figure 2L). Consistent with this observation, PCSK9<sup>liver(-/-)</sup> mice exhibited a significant reduction in the phosphorylation level of the AP-1 protein as compared to PCSK9<sup>liver(+/+)</sup> or PCSK9<sup>liver(+/-)</sup> mice ( $P < 0.001$ , Figure 2P).

## Effects of conditional knockdown of hepatic PCSK9 on MAPK and PI3K signaling pathways

Next, we investigated the alterations in hepatic MAPK and PI3K/AKT signaling pathways following hyperlipidemia challenge. As shown in Figures 3A–C, the PCSK9<sup>liver(-/-)</sup> mice group showed significant reductions in the mRNA expression of *p38-MAPK*, *ERK1/2*, and *JNK* by 29.5% ( $P < 0.05$ ), 59.6% ( $P < 0.01$ ), and 49.2% ( $P < 0.001$ ), respectively, as compared to that in the PCSK9<sup>liver(+/+)</sup> mice group. There were similar reductions in the expression of *p38-MAPK* and *ERK1/2*, but not *JNK*, in the PCSK9<sup>liver(+/-)</sup> mice group ( $P < 0.05$ ). Moreover, in both PCSK9<sup>liver(+/-)</sup> and PCSK9<sup>liver(-/-)</sup> mice groups, the levels of phosphorylated *p38-MAPK* and *ERK1/2* proteins were downregulated by approximately 60% ( $P < 0.01$ , Figure 3E) and 50% ( $P < 0.05$ , Figure 3F), respectively, as compared to those in the PCSK9<sup>liver(+/+)</sup> mice group. However, the levels of phosphorylated *JNK* exhibited no significant alterations among the mice groups (Figure 3G). Moreover, in PCSK9<sup>liver(-/-)</sup> mice, the gene expression of *PI3K* and *AKT* was decreased by 79.1% ( $P < 0.001$ ) and 58.6% ( $P < 0.05$ ), respectively, as compared to that in PCSK9<sup>liver(+/+)</sup> mice (Figures 3D, I). Consistent with this finding, in PCSK9<sup>liver(-/-)</sup> mice, the levels of phosphorylated *PI3K* and *AKT* proteins were downregulated by 60.8% ( $P < 0.01$ , Figure 3H) and 62.3% ( $P < 0.01$ , Figure 3J), respectively, as compared to those in PCSK9<sup>liver(+/+)</sup> mice.



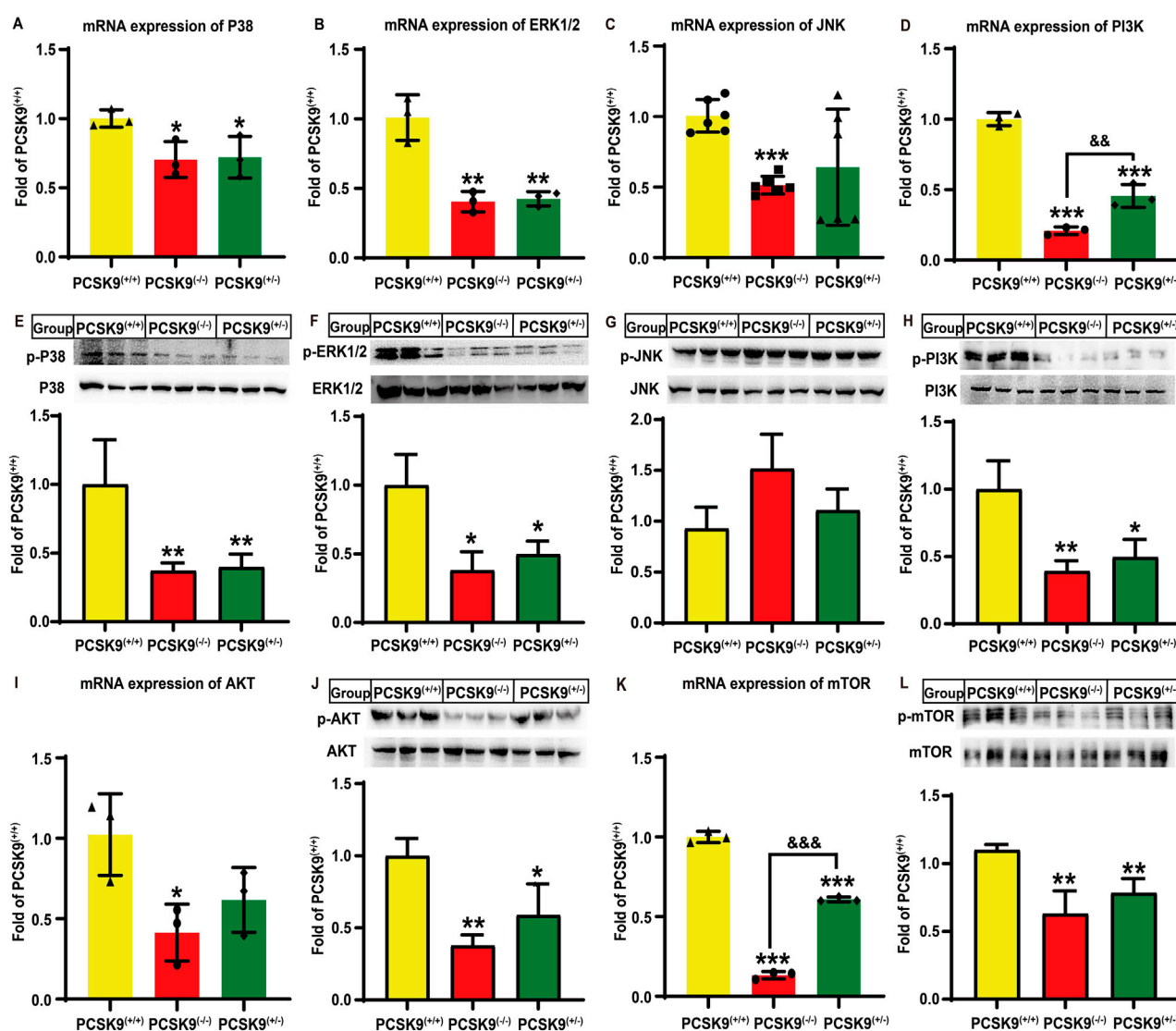


**FIGURE 3** Effects of conditional knockdown of hepatic PCSK9 on some molecules involved in the MAPK and PI3K/AKT signaling pathways in mice fed an HFD. Expression of (A), p38-MAPK (n = 3); (B), ERK1/2 (n = 3); (C), JNK (n = 6); and (D), PI3K (n = 3). Phosphorylated levels of (E), p38-MAPK; (F), ERK1/2; (G), JNK; and (H), PI3K proteins (n = 6). Expression of (I), AKT; and (K), mTOR (n = 3). Phosphorylated levels of (J), AKT; and (L), mTOR proteins (n = 6). \*means  $p < 0.05$  vs. PCSK9<sup>liver(+/-)</sup> group; \*\*means  $p < 0.01$  vs. PCSK9<sup>liver(+/-)</sup> group; \*\*\*means  $p < 0.001$  vs. PCSK9<sup>liver(+/-)</sup> group; &&& means  $p < 0.001$  vs. PCSK9<sup>liver(+/-)</sup> group.

Moreover, the mRNA expression of *PI3K* and *AKT* in PCSK9<sup>liver(+/-)</sup> mice was downregulated by 54.4% ( $P < 0.001$ ) and 38.3%, respectively, as compared to that in PCSK9<sup>liver(+/-)</sup> mice. Consistent with this finding, the levels of phosphorylated PI3K and AKT proteins in PCSK9<sup>liver(+/-)</sup> mice were decreased by 50.4% and 41.0%, respectively, as compared to those of PCSK9<sup>liver(+/-)</sup> mice ( $P < 0.05$ , Figures 3H, J). Additionally, PCSK9<sup>liver(+/-)</sup> and PCSK9<sup>liver(+/-)</sup> mice showed a reduction in mTOR expression levels by 86.7% ( $P < 0.001$ , Figure 3K) and 42.7% ( $P < 0.01$ , Figure 3L), respectively, as compared to that in PCSK9<sup>liver(+/-)</sup> mice. Consistent with this finding, the levels of phosphorylated mTOR protein were downregulated by approximately 39.2% ( $P < 0.001$ , Figure 3K) and 28.7% ( $P < 0.01$ , Figure 3L) in PCSK9<sup>liver(+/-)</sup> and PCSK9<sup>liver(+/-)</sup> mice, respectively.

## Effects of PCSK9 siRNA treatment on the inflammatory state of lipid-loaded HepG2 cells

Firstly, we demonstrated that the TC and TG levels in HepG2 cells were significantly increased after combined cis-9-octadecenoic acid and palmitic acid stimulation for 24 h, suggesting that a lipid-laden model was successfully established (Supplementary Figures S3A, B). Next, we demonstrated that lipid-loaded HepG2 cells exhibited higher levels of PCSK9, TNF $\alpha$ , IL-1 $\beta$ , IL-6, TLR-2, and TLR-4, and phosphorylated levels of NF- $\kappa$ B, MyD88, p38-MAPK, ERK1/2, JNK, PI3K, AKT, and mTOR proteins as compared to the blank control group. These findings suggested that lipid accumulation promoted inflammation

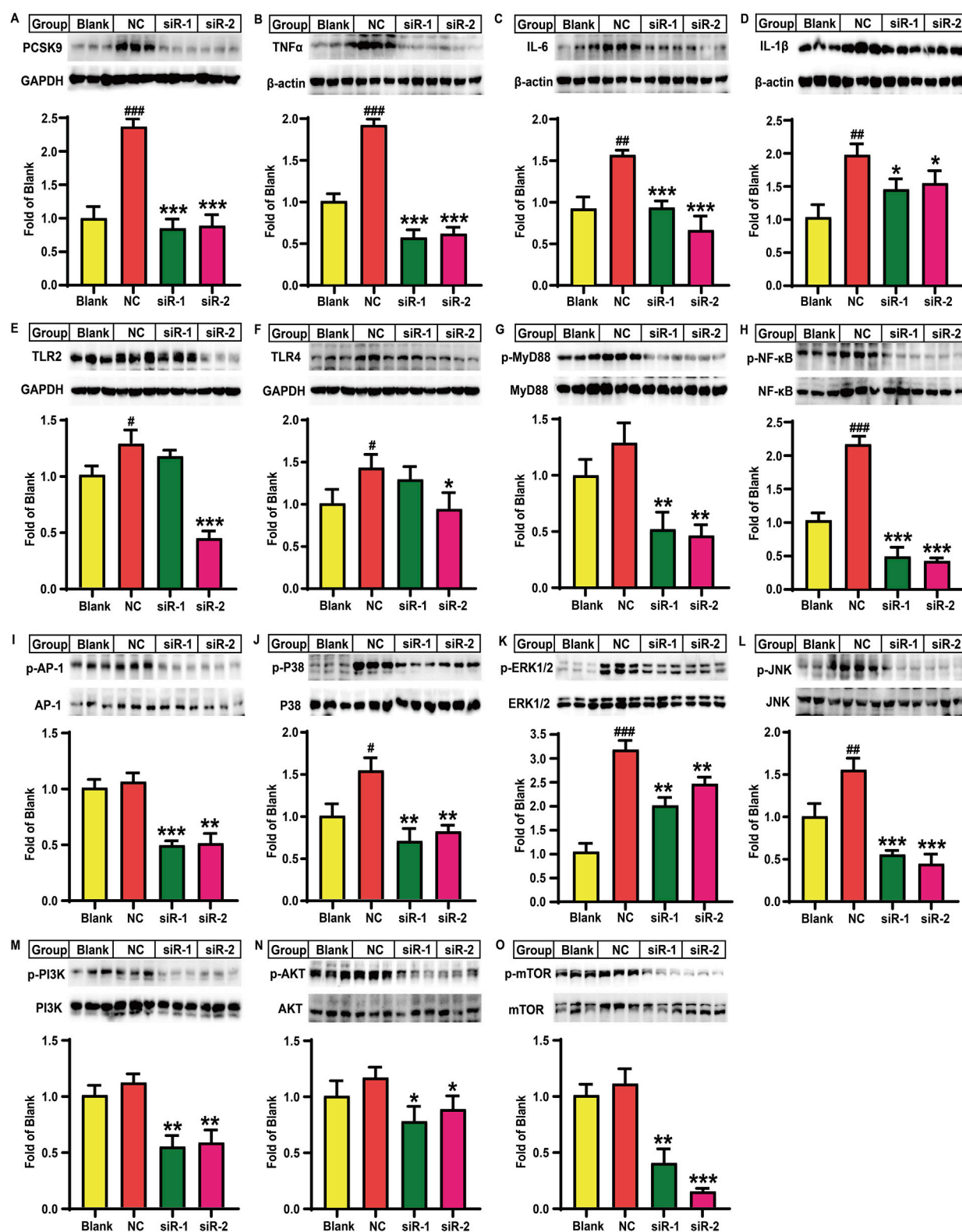


FIGURE 4

Effects of PCSK9 siRNA on the levels of some key molecules involved in lipid accumulation induced inflammation in HepG2 cells ( $n = 3$ ). Levels of (A), PCSK9; (B), TNFα; (C), IL-6; and (D), IL-1β; (E), TLR2; and (F), TLR4 proteins. Phosphorylated levels of (G), MyD88; (H), p65-NF-κB; (I), AP-1; (J), p38-MAPK; (K), ERK1/2; (L), JNK; (M), PI3K; (N), AKT; and (O), mTOR proteins. Blank: normal HepG2 cells; NC: lipid-loaded HepG2 cells were treated with negative control siRNA; siR-1: lipid-loaded HepG2 cells were treated with PCSK9 siRNA1; siR-2: lipid-loaded HepG2 cells were treated with PCSK9 siRNA2.

#means  $p < 0.05$  vs. Blank group; ##means  $p < 0.01$  vs. Blank group; ###means  $p < 0.001$  vs. Blank group; \*means  $p < 0.05$  vs. NC group; \*\*means  $p < 0.01$  vs. NC group; \*\*\*means  $p < 0.001$  vs. NC group.

in lipid-loaded HepG2 cells by regulating multiple signaling pathways as observed in mice. Importantly, there were no significant differences between the model and negative control groups, suggesting that the addition of control plasmid could not affect the levels of these proteins in lipid-loaded HepG2 cells (Supplementary Figure S3C–M and Supplementary Material S1). In the following, we investigated the effect of PCSK9 knockdown on lipid-loaded HepG2 cells and the underlying mechanisms of action. Lipid accumulation markedly increased the PCSK9 protein level by 136.2% ( $P < 0.001$ ) in the NC group, while siR-1 and siR-2 intervention groups significantly decreased the PCSK9 protein level ( $P < 0.001$ , Figure 4A), as compared to that in the blank control group; this finding confirmed the effectiveness of these two PCSK9 siRNAs. Notably, TNF $\alpha$ , IL-6, and IL-1 $\beta$  protein levels were remarkably increased in the NC group by approximately 91.3% ( $P < 0.001$ ), 70.4% ( $P < 0.01$ ), and 92.3% ( $P < 0.01$ ), respectively, as compared to those in the blank group, thus suggesting that lipid accumulation induced an inflammatory state in HepG2 cells. Compared to the NC group, the siR-1 intervention group showed a marked reduction in TNF $\alpha$ , IL-6, and IL-1 $\beta$  protein levels by 70.6% ( $P < 0.001$ ), 40.6% ( $P < 0.001$ ), and 26.5% ( $P < 0.05$ ), respectively, while the siR-2 intervention group reduced their levels by 68.2% ( $P < 0.001$ ), 57.9% ( $P < 0.001$ ), and 21.8% ( $P < 0.05$ ), respectively (Figures 4B–D). Lipid accumulation also elevated the TLR-2 and TLR-4 protein levels by approximately 40.0% and 53.5%, respectively, in the NC group ( $P < 0.05$ , Figures 4E, F). siR-2 alone significantly decreased TLR-2 and TLR-4 protein levels by 66.1% ( $P < 0.001$ ) and 34.5% ( $P < 0.05$ ), respectively. Although the NC group showed an increase by approximately 29.1% in the MyD88 protein phosphorylation level, this increase was not significant as compared to that in the blank group. In contrast, both siR-1 and siR-2 treatment significantly reduced MyD88 phosphorylation levels by approximately 60% as compared to that in the NC group ( $P < 0.01$ , Figure 4G). Notably, lipid accumulation in HepG2 cells significantly increased the p65 NF- $\kappa$ B protein phosphorylation level by 111.1% ( $P < 0.001$ , Figure 4H) without affecting AP-1 protein phosphorylation level as compared to that in the blank group (Figure 4I). However, transfection with siR-1 markedly decreased p65 NF- $\kappa$ B and AP-1 protein phosphorylation levels by approximately 77.6% ( $P < 0.001$ ) and 54.3% ( $P < 0.001$ ), respectively, while transfection with siR-2 decreased their levels by 80.9% ( $P < 0.001$ ) and 52.4% ( $P < 0.01$ ), respectively (Figures 4H, I), as compared to those in the NC group.

Additionally, as observed in the NC group, lipid accumulation significantly elevated p38-MAPK, ERK1/2, and JNK protein phosphorylation levels by 54.4% ( $P < 0.05$ ), 208.1% ( $P < 0.001$ ), and 55.5% ( $P < 0.01$ ), respectively, as compared to the blank control group (Figures 4J–L). In contrast, as compared to the NC group, both siR-1 and siR-2 for PCSK9 significantly decreased p38-MAPK, ERK1/2, and JNK protein phosphorylation levels by more than 47% ( $P < 0.01$ ), 23% ( $P < 0.01$ ), and 65% ( $P < 0.001$ ), respectively (Figures 4J–L). Lipid accumulation did not alter PI3K, AKT, and mTOR protein phosphorylation levels as compared to those in the blank control group (Figures 4M–O). However, as compared to the NC group, the siR-1 and siR-2 intervention groups showed a significant reduction in PI3K protein phosphorylation levels by 51.3% and 48.1%, respectively ( $P < 0.01$ , Figure 4M). siR-1 and siR-2 for PCSK9 also remarkably decreased the AKT protein

phosphorylation levels by approximately 33.6% and 24.1%, respectively ( $P < 0.05$ , Figure 4N). Additionally, the mTOR protein phosphorylation levels in the siR-1 and siR-2 treatment groups were reduced by 64.1% ( $P < 0.01$ ) and 87.3% ( $P < 0.001$ ), respectively, as compared to those in the NC group (Figure 4O).

## Effects of anti-PCSK9 antibody and/or p38-MAPK inhibitor on lipid-laden induced inflammation in HepG2 cells

Finally, we investigated the role of PCSK9 in lipid-laden HepG2 cells and the underlying mechanisms of action. As shown in Figure 5A, lipid accumulation increased PCSK9 protein levels by 20.5% ( $P < 0.01$ ) in HepG2 cells, while treatment of these cells with the anti-PCSK9 antibody alirocumab or the p38-MAPK inhibitor SB203580 alone or in combination significantly decreased PCSK9 protein levels by 65.3%, 69.6%, and 65.8%, as compared to those in the model group ( $P < 0.001$ ). Furthermore, compared to the blank control group, the model group showed an increase in the LDLR protein levels by 28.3%; however, neither alirocumab nor SB203580 significantly increased the LDLR protein level (Figure 5B). Notably, lipid accumulation significantly increased IL-6, IL-1 $\beta$ , and TNF $\alpha$  protein levels in the model group by approximately 52.7% ( $P < 0.01$ ), 174.6% ( $P < 0.001$ ), and 65.3% ( $P < 0.05$ ), respectively, in the model group as compared to those in the blank control group (Figures 5C–E), while alirocumab or SB203580 alone or in combination attenuated these changes. A noteworthy finding is that the IL-6 protein levels in the combination group were significantly reduced as compared to that in the alirocumab alone intervention group ( $P < 0.05$ , Figure 5C). TLR-4 and TLR-2 protein levels were significantly increased by 36.1% and 137.6%, respectively, in lipid-loaded HepG2 cells as compared to those in the blank control group ( $P < 0.01$ , Figures 5F,G). Intervention with anti-PCSK9 antibody significantly decreased TLR-4 level (~35.7%,  $P < 0.01$ ) and particularly TLR-2 level (~66.6%,  $P < 0.001$ ) in lipid-laden HepG2 cells. SB203580 exhibited similar effects as those observed for alirocumab. However, alirocumab addition following SB203580 intervention did not further decrease TLR-4 or TLR-2 protein levels. Moreover, lipid accumulation significantly increased the phosphorylated MyD88 protein level by 70.2% ( $P < 0.01$ ), while drug intervention significantly reversed this increase by approximately 65.9% ( $P < 0.001$ , Figure 5H). Importantly, alirocumab or SB203580 alone or in combination significantly decreased p65-NF- $\kappa$ B phosphorylation by approximately 36% ( $P < 0.05$ , Figure 5I) and reduced the phosphorylation levels of AP-1 by 61.0%, 75.5%, and 83.5%, respectively, as compared to those in the model group ( $P < 0.001$ , Figure 5J). The combination group showed a further decrease in the phosphorylated AP-1 protein level by 57.8% as compared to that in alirocumab alone intervention group ( $P < 0.01$ , Figure 5J).

Lipid accumulation also significantly increased the phosphorylation levels of p38-MAPK (~30.6%,  $P < 0.05$ , Figure 5K), ERK1/2 (~56.6%,  $P < 0.05$ , Figure 5L), and JNK (~59.9%,  $P < 0.01$ , Figure 5M) proteins, as compared to those of the blank control group. Furthermore, the p38-MAPK and JNK proteins, but not ERK1/2 protein, showed a decrease in the phosphorylation levels by 23.5% ( $P < 0.05$ ) and 26.6% ( $P < 0.05$ ),

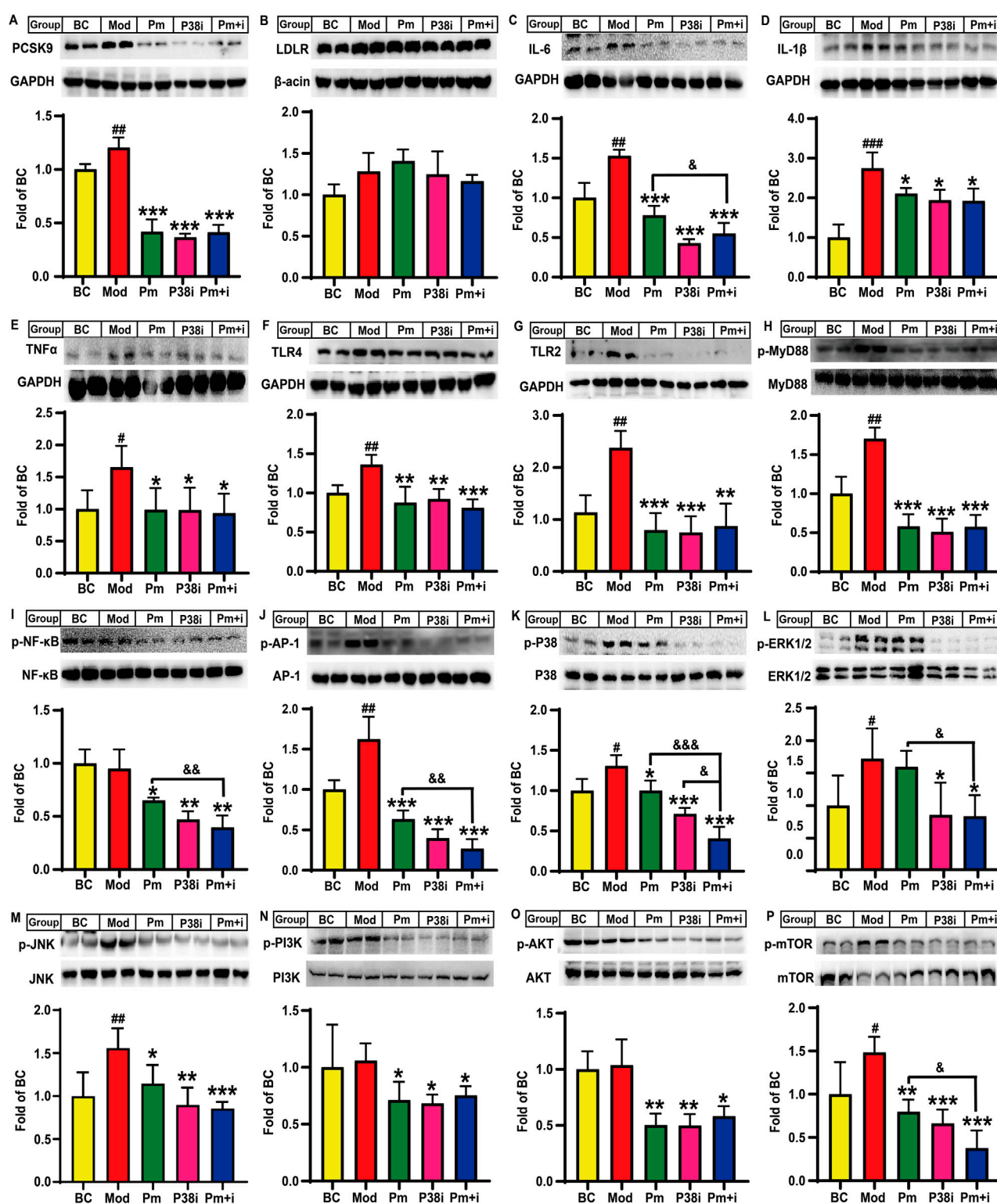


FIGURE 5

Effects of alirocumab and SB203580 on PCSK9, LDLR, and some key molecules involved in lipid accumulation induced inflammation in HepG2 cells ( $n = 4$ ). Levels of (A), PCSK9; (B), LDLR; (C), IL-6; (D), IL-1 $\beta$ ; (E), TNF $\alpha$ ; (F), TLR4; and (G), TLR2 proteins. Phosphorylated levels of (H), MyD88; (I), p65-NF- $\kappa$ B; (J), AP-1; (K), p38-MAPK; (L), ERK1/2; (M), JNK; (N), PI3K; (O), AKT; and (P), mTOR proteins. BC: blank control; Mod: model, lipid-loaded HepG2 cells; Pm: lipid-loaded HepG2 cells were treated with alirocumab (10  $\mu$ g/mL); p38i: lipid-loaded HepG2 cells were treated with SB203580 (30  $\mu$ M); Pm + i: combination group, lipid-loaded HepG2 cells were treated with PCSK9 alirocumab (10  $\mu$ g/mL) and SB203580 (30  $\mu$ M). # means  $p < 0.05$  vs. BC group; ## means  $p < 0.01$  vs. BC group; \*\*\* means  $p < 0.001$  vs. BC group; \* means  $p < 0.05$  vs. Mod group; \*\* means  $p < 0.01$  vs. Mod group; \*\*\* means  $p < 0.001$  vs. Mod group; & means  $p < 0.05$  vs. Pm + i group; && means  $p < 0.01$  vs. Pm + i group; &&& means  $p < 0.001$  vs. Pm + i group.



respectively, in the alirocumab alone intervention group as compared to that in the model group. As a positive control, SB203580 significantly reduced p38-MAPK, ERK1/2, and JNK phosphorylation levels by approximately 46.1% ( $P < 0.001$ , Figure 5K), 45.4% ( $P < 0.05$ , Figure 5L), and 42.5% ( $P < 0.01$ , Figure 5M), respectively, as compared to those in the model group. Notably, the combination group also exhibited a decrease in the p38-MAPK phosphorylation level as compared to the alirocumab alone intervention group ( $P < 0.001$ , Figure 5K). Moreover, alirocumab further reduced the p38-MAPK protein phosphorylation level by 42.9% following SB203580 administration ( $P < 0.05$ , Figure 5K); this finding suggests that the anti-PCSK9 antibody alirocumab showed a synergistic effect with the p38-MAPK inhibitor SB203580. Notably, the combination group displayed the best effect in reducing the JNK phosphorylation level as compared to the model group (~45.1%,  $P < 0.001$ , Figure 5M). Additionally, alirocumab or SB203580 alone or in combination remarkably decreased the phosphorylation levels of PI3K (~30%,  $P < 0.05$ ) and AKT (~50%,  $P < 0.05$ ) as compared to that in the model group (Figures 5N, O). Alirocumab, however, did not show a synergistic effect with SB203580 for reducing PI3K and AKT levels. Lipid accumulation in HepG2 cells also elevated the mTOR protein phosphorylation level by approximately 48.3% ( $P < 0.05$ ) as compared to that in the blank control. In contrast, alirocumab, SB203580, or their combination significantly decreased the mTOR protein phosphorylation levels by 46.2% ( $P < 0.01$ ), 55.3% ( $P < 0.001$ ), and 74.6% ( $P < 0.001$ ), respectively, as compared to those in the model group (Figure 5P). Furthermore, the combination intervention decreased the mTOR protein phosphorylation levels by 52.9% as compared to those in the alirocumab alone intervention group ( $P < 0.05$ , Figure 5P).

## Discussion

Recent studies have revealed that a positive association of PCSK9 with vascular inflammation (Tang et al., 2017; Yurtseven et al., 2020). Although PCSK9 deficiency in the liver elevates hepatic CD36-mediated fatty acid uptake, which increases the risk of liver injury and the expression of hepatic inflammatory factors, including IL-6, IL-1 $\beta$ , and TNF $\alpha$  (Demers et al., 2015; Lebeau et al., 2019), the effect of PCSK9 knockdown rather than its complete knockout on liver inflammation remains unclear. Here, we demonstrated that conditional knockdown of hepatic PCSK9 significantly decreased hyperlipidemia-induced gene expression and protein levels of some key pro-inflammatory factors potentially via downregulating several signaling pathways including TLR/MyD88, MAPK, and PI3K/AKT; this phenomenon further decreased the phosphorylation levels of NF- $\kappa$ B and AP-1 proteins in the nuclei, resulting in a reduction in inflammatory reaction.

First, we successfully obtained PCSK9<sup>liver(-/-)</sup>, PCSK9<sup>liver(+/-)</sup> and PCSK9<sup>liver(+/+)</sup> mice as confirmed by genotyping experiments. RT-qPCR and Western blotting assay showed a significant reduction in the gene expression and protein levels of PCSK9 in both PCSK9<sup>liver(-/-)</sup> and PCSK9<sup>liver(+/-)</sup> mice as compared to those in PCSK9<sup>liver(+/+)</sup> mice. In line with these observations, as a post-translational LDLR regulator, hepatic

PCSK9 knockdown apparently increased the LDLR protein level without affecting the gene expression of LDLR; these findings agreed with previously reported results (Maxwell and Breslow, 2004; Zhang et al., 2007; Zaid et al., 2008; Demers et al., 2015). In contrast, the downregulation of PCSK9 did not induce a significant increase in the LDLR protein level in HepG2 cells. Mechanistically, PCSK9 suppression has been demonstrated to downregulate SREBP-2 *in vitro*, a master regulator of LDLR and PCSK9 (Marques et al., 2022). Furthermore, the mice experimental groups showed no significant differences in body weight, liver indices, and hepatic TC levels. In line with these findings, the body weight and hepatic TC levels of PCSK9<sup>liver(+/+)</sup> and PCSK9<sup>liver(-/-)</sup> mice exhibited no significant difference after an HFD challenge for 12 weeks. However, PCSK9<sup>liver(-/-)</sup> mice displayed a significant increase in the liver indices accompanied with elevated levels of hepatic TG (approximately 90%) (Lebeau et al., 2019), and the hepatic TG levels were increased by 57.8% in PCSK9<sup>liver(-/-)</sup> mice as compared to that in PCSK9<sup>liver(+/+)</sup> mice due to elevated LDLR-mediated uptake of lipoprotein particles, especially non-HDL particles. These differences might be induced by the distinct challenge time (9 weeks vs. 12 weeks) and the difference in the hepatic PCSK9 levels (knockdown vs. knockout) between our study and the study of Lebeau (Lebeau et al., 2019). In hepatic-specific PCSK9 knockdown mice, the levels of hepatic PCSK9 proteins can be maintained at a certain level due to the following reasons. (1) Although PCSK9 is primarily expressed in the liver, this secretory protein is also generated by extrahepatic organs including colon, ileum, duodenum, and kidneys (Zaid et al., 2008); PCSK9 secreted by extrahepatic organs is transferred from the bloodstream to the liver. (2) Alb-Cre specifically target hepatocyte to knockout PCSK9, the rest cells, including hepatobiliary duct cell and Kupffer cell in the liver, still express PCSK9. These facts may explain why we did not observe significant differences in the levels of hepatic PCSK9 protein between PCSK9<sup>liver(-/-)</sup> and PCSK9<sup>liver(+/-)</sup> mice.

Second, we demonstrated that conditional knockdown of hepatic PCSK9 reduced hyperlipidemia-induced production of several pro-inflammatory cytokines (Figure 2, Supplementary Material S2, S3). Consistent with these findings, accumulating evidence has demonstrated that hyperlipidemia causes inflammation (Ma and Feng, 2016; Miao et al., 2023). For instance, familial hypercholesterolemia induces low-grade systemic inflammation, thereby promoting the onset and development of atherosclerosis, a chronic inflammatory disease. Anti-PCSK9 antibodies, such as alirocumab, reduce the levels of inflammatory cytokines in hypercholesterolemic patients (Marques et al., 2022; Seidah and Garçon, 2022). A Mendelian randomization study showed a positive association between the plasma TG levels and the increased risk of MAFLD (Chen et al., 2022). In the present study, the trend of reduction in plasma TC levels in PCSK9<sup>liver(-/-)</sup> and PCSK9<sup>liver(+/-)</sup> mice were consistent with previous findings (Zaid et al., 2008; Meng et al., 2023). As LDLR binds both apolipoprotein B and apolipoprotein E, conditional knockdown of hepatic PCSK9 not only reduced LDL-c levels but also decreased HDL-c levels, which were consistent with previous studies (Zaid et al., 2008; Meng et al., 2023). Importantly, both PCSK9<sup>liver(-/-)</sup> and PCSK9<sup>liver(+/-)</sup> mice exhibited a marked decrease in the gene expression and protein

levels of some hepatic pro-inflammatory cytokines such as IL-6, IL-1 $\beta$ , and TNF $\alpha$ . This reduction could be partially attributed to the decrease in circulating TC levels. However, the downregulation degree of these proinflammatory factors exhibited differences in PCSK9<sup>liver(-/-)</sup> and PCSK9<sup>liver(+/-)</sup> mice. For instance, the expression of TNF $\alpha$  was lower in PCSK9<sup>liver(+/-)</sup> mice as compared to that in PCSK9<sup>liver(-/-)</sup> mice, this may be partially attributed to the higher levels of hepatic TG in the latter. As the expression of these proinflammatory factors are modulated by a complex network, we cannot precisely explain these differences. In a mouse model of fibrosis, PCSK9 deletion alleviated hepatic inflammation, accompanied with a reduction in the plasma levels of lipopolysaccharide (LPS), aspartate aminotransferase (AST), and alanine aminotransferase (ALT), which are representative biomarkers of liver injury (Zou et al., 2020). Anti-PCSK9 monoclonal antibodies also lowered serum ALT and AST levels in some preclinical and clinical studies (Momtazi-Borojeni et al., 2022). Here, we found that alirocumab inhibited inflammation in lipid-loaded HepG2 cells. In another study, PCSK9 transgenic mice exhibited higher levels of liver injury, while PCSK9-deficient mice showed opposite effects, thus suggesting PCSK9 deficiency protects organs against bacterial dissemination and inflammatory injury (Dwivedi et al., 2016). However, the related mechanisms are not yet known. Another noteworthy finding is that PCSK9 knockdown ameliorates aortic inflammation by inhibiting the TLR-4 signaling pathway without affecting the lipid profiles in apolipoprotein E-deficient mice (Tang et al., 2017). These findings imply that PCSK9 inhibition may directly suppress inflammation through mechanisms other than lowering of the lipid level.

Third, our results suggest that conditional knockdown of hepatic PCSK9 ameliorates hyperlipidemia-induced inflammation by downregulating multiple signaling pathways. Here, we showed that conditional knockdown of hepatic PCSK9 or intervention with anti-PCSK9 antibody significantly decreased TLR-4 expression levels both *in vivo* and *in vitro*. LPS is an endotoxin recognized by TLR-4 localized on the membrane of several cell types, including hepatocytes (Lee et al., 2021). Several previous studies suggest that PCSK9 knockdown inhibits TLR-4/Myd88/NF- $\kappa$ B signaling in the aorta of apolipoprotein E-deficient mice or rabbits (Tang et al., 2017; Liu et al., 2020). Mechanistically, the unique C-terminal cysteine-rich domain of PCSK9 is presumed to bind and activate TLR-4, thereby causing an inflammatory reaction (Tarkowski et al., 2010; Cheng et al., 2016; Tang et al., 2017). These findings indicate that PCSK9 in different organs or cells might induce inflammation by modulating of the same TLR-4 signaling pathway. In contrast, our results demonstrated that hepatic PCSK9 knockdown or inhibition particularly reduced TLR-2 level rather than TLR-4 level, with inhibition of the downstream NF- $\kappa$ B and AP-1 signaling pathways, thus suggesting PCSK9 suppression may stimulate different TLR family members following hyperlipidemia challenge. Lipid accumulation may also induce other unknown proinflammatory factors, apart from LPS, which participate in TLR-2 activation. It is necessary to note that PCSK9<sup>liver(-/-)</sup> and PCSK9<sup>liver(+/-)</sup> mice exhibited different effect on suppressing the gene expression and protein levels of phosphorylated AP-1, suggesting the slight differences in the levels of PCSK9 may play a key role in

modulating this transcription factor. The downregulation of the proinflammatory factors in PCSK9<sup>liver(+/-)</sup> mice may primarily attribute to the downregulation of NF- $\kappa$ B and other unknown transcription factors.

Notably, recent studies have indicated a relationship between PCSK9 and the MAPK signaling pathway. A microarray analysis suggested that a gain-of-function mutation in PCSK9 (D374Y) increases the expression of several signaling molecules involved in inflammation, including TNF- $\alpha$ , TNF receptor IIa, MAPK kinase, and NF- $\kappa$ B in HepG2 cells (Lan et al., 2010). Another study demonstrated that MAPKs, including ERK, JNK, and p38-MAPK, are involved in PCSK9 secretion, particularly in mice fed an HFD (Ding et al., 2020b). Our findings indicated that conditional knockdown of hepatic PCSK9 *in vivo* or PCSK9 suppression *in vitro* inhibited the phosphorylation of ERK1/2 and p38-MAPK proteins involved in the MAPK signaling pathway. However, PCSK9 suppression exhibited differences in modulation of JNK *in vivo* and *in vitro*. This may be explained by the different modulatory mechanisms because the *in vivo* situations are more complexed than those *in vitro*. Moreover, the alterations of the mRNA expression of these MAPKs were inconsistent with their protein levels, suggesting some unknown mechanisms are involved in the post-translational regulation of these proteins. For instance, the levels of protein are finely controlled by multiple factors, including the stability of mRNA, the function of ribosome, the levels of translation-related factors, and protein degradation (Wu and Bazzini, 2023; Jia et al., 2024). In this study, alirocumab further decreased the phosphorylation level of the p38-MAPK protein; however, it did not affect IL-6, IL-1 $\beta$ , and TNF $\alpha$  proinflammatory cytokine levels following treatment with the p38-MAPK inhibitor *in vitro*. This result indicates that the p38-MAPK signaling pathway may primarily contribute to PCSK9-mediated inflammation in lipid-loaded HepG2 cells. In addition to ERK1/2 and p38-MAPK proteins, JNK protein phosphorylation level was reduced by PCSK9 siRNAs, thus suggesting that PCSK9 siRNAs showed more robust effects in inhibiting the MAPK signaling pathway than alirocumab. Consistent with this observation, a recent study demonstrated that downregulation of the MAPK signaling pathway is a protective mechanism for MASH (Wu et al., 2023). All these findings suggest that the mechanisms of action of PCSK9 suppression on attenuating hyperlipidemia-induced inflammation are associated with downregulation of the MAPK signaling pathway.

Several previous studies have also indicated an association between the PI3K/AKT signaling pathway and PCSK9. For instance, PI3K/AKT signaling is involved in modulating the sterol regulatory element binding protein-2/PCSK9 signaling pathway in HepG2 cells (Xiao et al., 2019). Here, we found that conditional knockdown of hepatic PCSK9 suppressed the levels of phosphorylated PI3K, AKT, NF- $\kappa$ B, and AP-1 proteins following hyperlipidemia challenge; this result suggests that PCSK9 knockdown may reduce inflammation by inhibiting the PI3K/AKT signaling pathway. Another study also indicated that PCSK9 deficiency suppresses AKT protein phosphorylation in hyperlipidemic mice (Lebeau et al., 2019). mTOR, a downstream molecule of the PI3K/AKT signaling pathway, is involved in modulating autophagy, a cellular protective mechanism following

unfavorable conditions such as inflammation (Yurtseven et al., 2020; Rajendran et al., 2024). Interestingly, PCSK9 inhibition promotes autophagy by suppressing phosphorylation of mTOR (Ding et al., 2016; Yurtseven et al., 2020). Our results demonstrated that hepatic PCSK9 knockdown *in vivo* or PCSK9 inhibition *in vitro* markedly reduced phosphorylated mTOR levels, thus suggesting that PCSK9 suppression may attenuate inflammation by improving autophagy. It is worth noting that HFD-induced upregulation of the PI3K/AKT signaling pathway in mice cannot be reproduced in lipid-loaded HepG2 cells potentially due to the distinct metabolic situations of these two models. However, both anti-PCSK9 antibody and siRNAs against PCSK9 significantly inhibited the PI3K/AKT/mTOR signaling pathway in HepG2 cells as observed in PCSK9<sup>liver(-/-)</sup> and PCSK9<sup>liver(+/-)</sup> mice.

Although the complete deletion of PCSK9, an extreme condition, enhanced CD36-mediated lipid accumulation and subsequent inflammation in mice (Demers et al., 2015; Lebeau et al., 2019), our findings revealed that conditional knockdown of hepatic PCSK9 *in vivo* and PCSK9 suppression *in vitro* were associated with decreased inflammation following lipid accumulation. These contrasting results might be due to the abovementioned reasons, including differences in the animal model (PCSK9-deficient model vs. conditional knockdown of hepatic PCSK9 model), HFD challenge period (12 weeks vs. 9 weeks), and the differences in the components of HFD. In our model, PCSK9 secreted by other organs is transferred to liver through blood flow and exert its effects, such as downregulation of CD36, thereby partially ameliorating hepatic lipid accumulation. Moreover, a shorter challenge period in our study may reduce the severity of hepatic lipid accumulation. These assumptions are consistent with the unaltered liver indices and less hepatic TG accumulation noted in our study. Consistent with this finding, PCSK9 overexpression or gain-of-function exhibited an association with MAFLD as revealed by laboratory and clinical studies (Lebeau et al., 2022). These observations suggest that PCSK9 modulation may induce different or even contrasting complementary mechanisms under distinct conditions. For instance, PCSK9-deficient mice exhibit higher levels of ATP-binding cassette transporter A1 and higher levels of cholesterol in the feces than control mice; this suggests that PCSK9 deletion may promote reverse cholesterol transport as a complementary mechanism (Lebeau et al., 2019). Moreover, PCSK9<sup>liver(-/-)</sup> mice showed impairment of liver regeneration, while PCSK9<sup>liver(+/-)</sup> mice exhibit an improved liver regeneration and resistance to hepatic steatosis (Momtazi-Borojeni et al., 2022); this finding indicates that a moderate level of the PCSK9 protein can protect mice against MAFLD and MASH. As discussed above, although hyperlipidemia causes inflammation, it remains unclear how excessive hepatic lipid accumulation may promote elevated production of proinflammatory factors, thereby inducing systemic inflammation (Ugovšek and Šebešćen, 2022). An appropriate elevated level of hepatic TG accumulation may stimulate complementary anti-inflammatory mechanisms. It should also be noted that conditional knockdown of hepatic PCSK9 significantly decreased plasma TC levels, which are sure to ameliorate systemic inflammation and thereby reduce hepatic inflammation.

In conclusion, the results of the present study suggest that PCSK9 downregulation to ameliorates hyperlipidemia-induced liver inflammation without inducing severe lipid accumulation. The related mechanisms of action are associated with the downregulation of TLR-4, TLR-2, MAPK, and PI3K/AKT/mTOR as well as their downstream NF-κB and AP-1 signaling pathways. However, this study has several limitations as mentioned hereafter. Firstly, in the liver of PCSK9<sup>liver(+/-)</sup> and PCSK9<sup>liver(-/-)</sup> mice, there is PCSK9 expressed by other cells and transferred from the blood flow as discussed above. Therefore, complete knockout of hepatic PCSK9 is not available, and we only demonstrated that hepatic PCSK9 knockdown attenuates hyperlipidemia-induced liver inflammation. A comparative study is necessary to confirm the differences in HFD-induced chronic liver inflammation by using PCSK9 knockout and hepatic PCSK9 knockdown animal models. Secondly, HepG2 cells are derived from human liver carcinoma and their metabolic profiles often differ significantly from normal hepatocytes. Furthermore, the *in vivo* anti-inflammatory mechanisms are more complex than those *in vitro*. Therefore, some of the *in vivo* results in PCSK9 knockdown mice, including the regulation of the PI3K/AKT signaling pathway and PCSK9-mediated LDLR degradation, could not be reproduced in HepG2 cells in this study. Thus, it is necessary to determine whether siRNAs or antibodies against PCSK9 could reduce lipid accumulation induced inflammation in primary hepatocytes. Furthermore, we only investigated the anti-inflammatory effects of PCSK9 antibody (alirocumab) and siRNAs in HepG2 cells pre-loaded with lipids. Although this model is designed to mimic MAFLD therapy using PCSK9 inhibitors, these experiments cannot reflect the effects of PCSK9 suppression induced increase in LDLR-mediated lipid uptake, which might affect the final anti-inflammatory effects of PCSK9 inhibition. Additionally, the effects of PCSK9 on modulation of lipid metabolism in HepG2 cells, especially the underlying mechanisms of action are not well clarified. Thirdly, although we investigated the effects of conditional knockdown of hepatic PCSK9 on HFD-induced liver inflammation following 3-month intervention and the underlying mechanisms of action, this study cannot reflect the potential different effects of PCSK9 in the dynamic processes of hyperlipidemia-induced liver inflammation. Furthermore, as PCSK9<sup>liver(-/-)</sup> mice with a minor higher level of liver TG exhibited equal or even stronger anti-inflammatory effects as compared to those in PCSK9<sup>liver(+/-)</sup> or PCSK9<sup>liver(+/-)</sup> mice, it remains to be determined how excessive hepatic lipid accumulation may cause elevated liver inflammation or MASH in mice with conditional knockdown of hepatic PCSK9. Fourth, because multiple signaling pathways are involved in these processes, we could not presently confirm the contribution of each signaling pathway. Furthermore, whether PCSK9 differently regulate the JNK, p38-MAPK, and ERK signaling pathways requires further studies in the future.

## Data availability statement

The original contributions presented in the study are included in the article/Supplementary Material, further inquiries can be directed to the corresponding author.

## Ethics statement

The animal study was approved by Laboratory Animal Ethical Committee of Shandong Second Medical University (2020SDL106). The study was conducted in accordance with the local legislation and institutional requirements.

## Author contributions

X-YZ: Data curation, Formal Analysis, Investigation, Writing—original draft. Q-QL: Methodology, Resources, Software, Writing—original draft. Y-JL: Funding acquisition, Methodology, Project administration, Supervision, Writing—review and editing. S-RS: Formal Analysis, Investigation, Writing—original draft. C-NM: Formal Analysis, Investigation, Writing—original draft. MM: Data curation, Formal Analysis, Investigation, Writing—original draft. S-DG: Funding acquisition, Resources, Supervision, Writing—review and editing.

## Funding

The author(s) declare that financial support was received for the research, authorship, and/or publication of this article. This work was supported by National Natural Science Foundation of China (82070469).

## References

- Andreaddou, I., Tsoumani, M., Vilahur, G., Ikonomidis, I., Badimon, L., Varga, Z. V., et al. (2020). PCSK9 in myocardial infarction and cardioprotection: importance of lipid metabolism and inflammation. *Front. Physiol.* 11, 602497. doi:10.3389/fphys.2020.602497
- Badimon, L., Luquero, A., Crespo, J., Peña, E., and Borrell-Pages, M. (2021). PCSK9 and LRP5 in macrophage lipid internalization and inflammation. *Cardiovasc. Res.* 117, 2054–2068. doi:10.1093/cvr/cvaa254
- Baginski, A. M., Farmer, N., Baumer, Y., Wallen, G. R., and Powell-Wiley, T. M. (2022). Interleukin-8 (IL-8) as a potential mediator of an association between trimethylamine n-oxide (TMAO) and proprotein convertase subtilisin/kexin type 9 (PCSK9) among African Americans at risk of cardiovascular disease. *Metabolites* 12, 1196. doi:10.3390/metabo12121196
- Chen, J., Zhou, H., Jin, H., and Liu, K. (2022). Role of inflammatory factors in mediating the effect of lipids on nonalcoholic fatty liver disease: a two-step, multivariable mendelian randomization study. *Nutrients* 14, 4434. doi:10.3390/nu14204434
- Cheng, J. M., Oemrawsingh, R. M., Garcia-Garcia, H. M., Boersma, E., van Geuns, R. J., Serruys, P. W., et al. (2016). PCSK9 in relation to coronary plaque inflammation: results of the ATHEROREMO-IVUS study. *Atherosclerosis* 248, 117–122. doi:10.1016/j.atherosclerosis.2016.03.010
- Coppinger, C., Movahed, M. R., Azemawah, V., Peyton, L., Gregory, J., and Hashemzadeh, M. (2022). A comprehensive review of PCSK9 inhibitors. *J. Cardiovasc. Pharmacol. Ther.* 27, 10742484221100107. doi:10.1177/10742484221100107
- Demers, A., Samami, S., Lauzier, B., Des Rosiers, C., Ngo Sock, E. T., Ong, H., et al. (2015). PCSK9 induces CD36 degradation and affects long-chain fatty acid uptake and triglyceride metabolism in adipocytes and in mouse liver. *Arterioscler. Thromb. Vasc. Biol.* 35, 2517–2525. doi:10.1161/ATVBAHA.115.306032
- Deng, S. J., Shen, Y., Gu, H. M., Guo, S., Wu, S. R., and Zhang, D. W. (2020). The role of the C-terminal domain of PCSK9 and SEC24 isoforms in PCSK9 secretion. *Biochim. Biophys. Acta Mol. Cell Biol. Lipids* 1865, 158660. doi:10.1016/j.bbalip.2020.158660
- Ding, Z., Liu, S., Wang, X., Mathur, P., Dai, Y., Theus, S., et al. (2016). Cross-talk between PCSK9 and damaged mtDNA in vascular smooth muscle cells: role in apoptosis. *Antioxid. Redox Signal.* 25, 997–1008. doi:10.1089/ars.2016.6631
- Ding, Z., Pothineni, N. V. K., Goel, A., Lüscher, T. F., and Mehta, J. L. (2020a). PCSK9 and inflammation: role of shear stress, pro-inflammatory cytokines, and LOX-1. *Cardiovasc. Res.* 116, 908–915. doi:10.1093/cvr/cvz313
- Ding, Z., Wang, X., Liu, S., Zhou, S., Kore, R. A., Mu, S., et al. (2020b). NLRP3 inflammasome via IL-1 $\beta$  regulates PCSK9 secretion. *Theranostics* 10, 7100–7110. doi:10.7150/thno.45939
- Dixon, D. L., Trankle, C., Buckley, L., Parod, E., Carbone, S., Van Tassell, B. W., et al. (2016). A review of PCSK9 inhibition and its effects beyond LDL receptors. *J. Clin. Lipidol.* 10, 1073–1080. doi:10.1016/j.jacl.2016.07.004
- Dwivedi, D. J., Grin, P. M., Khan, M., Prat, A., Zhou, J., Fox-Robichaud, A. E., et al. (2016). Differential expression of PCSK9 modulates infection, inflammation, and coagulation in a murine model of sepsis. *Shock* 46, 672–680. doi:10.1097/SHK.0000000000000682
- Fang, Z., Shen, G., Wang, Y., Hong, F., Tang, X., Zeng, Y., et al. (2024). Elevated Kallistatin promotes the occurrence and progression of non-alcoholic fatty liver disease. *Signal Transduct. Target. Ther.* 9, 66. doi:10.1038/s41392-024-01781-9
- Ferri, N., and Ruscica, M. (2016). Proprotein convertase subtilisin/kexin type 9 (PCSK9) and metabolic syndrome: insights on insulin resistance, inflammation, and atherogenic dyslipidemia. *Endocrine* 54, 588–601. doi:10.1007/s12020-016-0939-0
- Fu, Y. J., Xu, B., Huang, S. W., Luo, X., Deng, X. L., Luo, S., et al. (2021). Baicalin prevents LPS-induced activation of TLR4/NF- $\kappa$ B p65 pathway and inflammation in mice via inhibiting the expression of CD14. *Acta Pharmacol. Sin.* 42, 88–96. doi:10.1038/s41401-020-0411-9
- Jia, X., He, X., Huang, C., Li, J., Dong, Z., and Liu, K. (2024). Protein translation: biological processes and therapeutic strategies for human diseases. *Signal Transduct. Target. Ther.* 9, 44. doi:10.1038/s41392-024-01749-9
- Keeter, W. C., Carter, N. M., Nadler, J. L., and Galkina, E. V. (2022). The AAV-PCSK9 murine model of atherosclerosis and metabolic dysfunction. *Eur. Heart J. Open* 2, oead028. doi:10.1093/ehjopen/oead028
- Lan, H., Pang, L., Smith, M. M., Levitan, D., Ding, W., Liu, L., et al. (2010). Proprotein convertase subtilisin/kexin type 9 (PCSK9) affects gene expression pathways beyond cholesterol metabolism in liver cells. *J. Cell. Physiol.* 224, 273–281. doi:10.1002/jcp.22130

## Conflict of interest

The authors declare that the research was conducted in the absence of any commercial or financial relationships that could be construed as a potential conflict of interest.

## Generative AI statement

The author(s) declare that no Generative AI was used in the creation of this manuscript.

## Publisher's note

All claims expressed in this article are solely those of the authors and do not necessarily represent those of their affiliated organizations, or those of the publisher, the editors and the reviewers. Any product that may be evaluated in this article, or claim that may be made by its manufacturer, is not guaranteed or endorsed by the publisher.

## Supplementary material

The Supplementary Material for this article can be found online at: <https://www.frontiersin.org/articles/10.3389/fphar.2025.1528250/full#supplementary-material>



- Lebeau, P. F., Byun, J. H., Platko, K., Al-Hashimi, A. A., Lhoták, Š., MacDonald, M. E., et al. (2019). Pcsk9 knockout exacerbates diet-induced non-alcoholic steatohepatitis, fibrosis and liver injury in mice. *JHEP Rep.* 1, 418–429. doi:10.1016/j.jhepr.2019.10.009
- Lebeau, P. F., Platko, K., Byun, J. H., Makda, Y., and Austin, R. C. (2022). The emerging roles of intracellular PCSK9 and their implications in endoplasmic reticulum stress and metabolic diseases. *Metabolites* 12, 215. doi:10.3390/metabo12030215
- Lee, J. S., O'Connell, E. M., Pacher, P., and Lohoff, F. W. (2021). PCSK9 and the gut-liver-brain axis: a novel therapeutic target for immune regulation in alcohol use disorder. *J. Clin. Med.* 10, 1758. doi:10.3390/jcm10081758
- Li, T., Hu, S. M., Pang, X. Y., Wang, J. F., Yin, J. Y., Li, F. H., et al. (2020). The marine-derived furanone reduces intracellular lipid accumulation *in vitro* by targeting LXRA and PPARα. *J. Cell. Mol. Med.* 24, 3384–3398. doi:10.1111/jcmm.15012
- Li, Y., Miao, M., Yin, F., Shen, N., Yu, W. Q., and Guo, S. D. (2022). The polysaccharide-peptide complex from mushroom *Cordyceps militaris* ameliorates atherosclerosis by modulating the lncRNA-miRNA-mRNA axis. *Food Funct.* 13, 3185–3197. doi:10.1039/d1fo03285b
- Liu, S., Deng, X., Zhang, P., Wang, X., Fan, Y., Zhou, S., et al. (2020). Blood flow patterns regulate PCSK9 secretion via MyD88-mediated pro-inflammatory cytokines. *Cardiovasc. Res.* 116, 1721–1732. doi:10.1093/cvr/cvz262
- Low, L. D., Lu, L., Chan, C. Y., Chen, J., Yang, H. H., Yu, H., et al. (2020). IL-13-driven alterations in hepatic cholesterol handling contributes to hypercholesterolemia in a rat model of minimal change disease. *Clin. Sci.* 134, 225–237. doi:10.1042/CS20190961
- Ma, X., and Feng, Y. (2016). Hypercholesterolemia tunes hematopoietic stem/progenitor cells for inflammation and atherosclerosis. *Int. J. Mol. Sci.* 17, 1162. doi:10.3390/ijms17071162
- Marques, P., Domingo, E., Rubio, A., Martínez-Hervás, S., Ascaso, J. F., Piqueras, L., et al. (2022). Beneficial effects of PCSK9 inhibition with alirocumab in familial hypercholesterolemia involve modulation of new immune players. *Biomed. Pharmacother.* 145, 112460. doi:10.1016/j.biopha.2021.112460
- Maxwell, K. N., and Breslow, J. L. (2004). Adenoviral-mediated expression of Pcsk9 in mice results in a low-density lipoprotein receptor knockout phenotype. *Proc. Natl. Acad. Sci. U. S. A.* 101, 7100–7105. doi:10.1073/pnas.0402133101
- Meng, F. H., Liu, S., Xiao, J., Zhou, Y. X., Dong, L. W., Li, Y. F., et al. (2023). New loss-of-function mutations in PCSK9 reduce plasma LDL cholesterol. *Arterioscler. Thromb. Vasc. Biol.* 43, 1219–1233. doi:10.1161/ATVBAHA.123.318839
- Miao, M., Wang, X., Liu, T., Li, Y. J., Yu, W. Q., Yang, T. M., et al. (2023). Targeting PPARs for therapy of atherosclerosis: a review. *Int. J. Biol. Macromol.* 242, 125008. doi:10.1016/j.ijbiomac.2023.125008
- Momtazi-Borojeni, A. A., Banach, M., Ruscica, M., and Sahebkar, A. (2022). The role of PCSK9 in NAFLD/NASH and therapeutic implications of PCSK9 inhibition. *Expert Rev. Clin. Pharmacol.* 15, 1199–1208. doi:10.1080/17512433.2022.2132229
- Peled, M., Nishi, H., Weinstock, A., Barrett, T. J., Zhou, F., Quezada, A., et al. (2017). A wild-type mouse-based model for the regression of inflammation in atherosclerosis. *PLOS ONE* 12, e0173975. doi:10.1371/journal.pone.0173975
- Punch, E., Klein, J., Diaba-Nuhoho, P., Morawietz, H., and Garelnabi, M. (2022). Effects of PCSK9 targeting: alleviating oxidation, inflammation, and atherosclerosis. *J. Am. Heart Assoc.* 11, e023328. doi:10.1161/JAHA.122.023328
- Rajendran, P., Sekar, R., Dhayasankar, P. S., Ali, E. M., Abdelsalam, S. A., Balaraman, S., et al. (2024). PI3K/AKT signaling pathway mediated autophagy in oral carcinoma - a comprehensive review. *Int. J. Med. Sci.* 21, 1165–1175. doi:10.7150/ijms.94566
- Seidah, N. G., and Garçon, D. (2022). Expanding biology of PCSK9: roles in atherosclerosis and beyond. *Curr. Atheroscler. Rep.* 24, 821–830. doi:10.1007/s11883-022-01057-z
- Tang, Z., Jiang, L., Peng, J., Ren, Z., Wei, D., Wu, C., et al. (2012). PCSK9 siRNA suppresses the inflammatory response induced by oxLDL through inhibition of NF-κB activation in THP-1-derived macrophages. *Int. J. Mol. Med.* 30, 931–938. doi:10.3892/ijmm.2012.1072
- Tang, Z. H., Peng, J., Ren, Z., Yang, J., Li, T. T., Li, T. H., et al. (2017). New role of PCSK9 in atherosclerotic inflammation promotion involving the TLR4/NF-κB pathway. *Atherosclerosis* 262, 113–122. doi:10.1016/j.atherosclerosis.2017.04.023
- Tarkowski, A., Bjersing, J., Shestakov, A., and Bokarewa, M. I. (2010). Resistin competes with lipopolysaccharide for binding to toll-like receptor 4. *J. Cell. Mol. Med.* 14, 1419–1431. doi:10.1111/j.1582-4934.2009.00899.x
- Tran, S., Baba, I., Poupel, L., Dussaud, S., Moreau, M., Gelineau, A., et al. (2020). Impaired kupffer cell self-renewal alters the liver response to lipid overload during non-alcoholic steatohepatitis. *Immunity* 53, 627–640. doi:10.1016/j.immuni.2020.06.003
- Ugovšek, S., and Šebešljen, M. (2022). Non-lipid effects of PCSK9 monoclonal antibodies on vessel wall. *J. Clin. Med.* 11, 3625. doi:10.3390/jcm11133625
- Wu, Q., and Bazzini, A. A. (2023). Translation and mRNA stability control. *Annu. Rev. Biochem.* 92, 227–245. doi:10.1146/annurev-biochem-052621-091808
- Wu, T., Chen, X., Xu, K., Dai, C., Li, X., Zhang, Y. W. Q., et al. (2023). LIM domain only 7 negatively controls nonalcoholic steatohepatitis in the setting of hyperlipidemia. *Hepatology* 79, 149–166. doi:10.1097/HEP.0000000000000585
- Xiao, J., Bai, X. Q., Liao, L., Zhou, M., Peng, J., Xiang, Q., et al. (2019). Hydrogen sulfide inhibits PCSK9 expression through the PI3K/Akt-SREBP-2 signaling pathway to influence lipid metabolism in HepG2 cells. *Int. J. Mol. Med.* 43, 2055–2063. doi:10.3892/ijmm.2019.4118
- Yang, Z., Yin, J., Wang, Y., Wang, J., Xia, B., Li, T., et al. (2019). The fucoidan A3 from the seaweed *Ascophyllum nodosum* enhances RCT-related genes expression in hyperlipidemic C57BL/6J mice. *Int. J. Biol. Macromol.* 134, 759–769. doi:10.1016/j.ijbiomac.2019.05.070
- Yin, J., Wang, J., Li, F., Yang, Z., Yang, X., Sun, W., et al. (2019). The fucoidan from the brown seaweed *Ascophyllum nodosum* ameliorates atherosclerosis in apolipoprotein E-deficient mice. *Food Funct.* 10, 5124–5139. doi:10.1039/c9fo00619b
- Yurtseven, E., Ural, D., Baysal, K., and Tokgözoğlu, L. (2020). An update on the role of PCSK9 in atherosclerosis. *J. Atheroscler. Thromb.* 27, 909–918. doi:10.5551/jat.55400
- Zaid, A., Roubtsova, A., Essalmani, R., Marcinkiewicz, J., Chamberland, A., Hamelin, J., et al. (2008). Proprotein convertase subtilisin/kexin type 9 (PCSK9): hepatocyte-specific low-density lipoprotein receptor degradation and critical role in mouse liver regeneration. *Hepatology* 48, 646–654. doi:10.1002/hep.22354
- Zhang, D. W., Lagace, T. A., Garuti, R., Zhao, Z., McDonald, M., Horton, J. D., et al. (2007). Binding of proprotein convertase subtilisin/kexin type 9 to epidermal growth factor-like repeat A of low density lipoprotein receptor decreases receptor recycling and increases degradation. *J. Biol. Chem.* 282, 18602–18612. doi:10.1074/jbc.M702027200
- Zhang, X., Xu, H., Yu, J., Cui, J., Chen, Z., Li, Y., et al. (2023). Immune regulation of the liver through the PCSK9/CD36 pathway during heart transplant rejection. *Circulation* 148, 336–353. doi:10.1161/CIRCULATIONAHA.123.062788
- Zhang, Y., Jia, X. B., Liu, Y. C., Yu, W. Q., Si, Y. H., and Guo, S. D. (2022). Fenofibrate enhances lipid deposition via modulating PPARγ, SREBP-1c, and gut microbiota in *ob/ob* mice fed a high-fat diet. *Front. Nutr.* 9, 971581. doi:10.3389/fnut.2022.971581
- Zhang, Y., Wei, S., Zhang, Q., Zhang, Y., and Sun, C. (2024). Paris saponin VII inhibits triple-negative breast cancer by targeting the MEK/ERK/STMN1 signaling axis. *Phytomedicine* 130, 155746. doi:10.1016/j.phymed.2024.155746
- Zhao, Y., Liu, L., Yang, S., Liu, G., Pan, L., Gu, C., et al. (2021). Mechanisms of atherosclerosis induced by postprandial lipemia. *Front. Cardiovasc. Med.* 8, 636947. doi:10.3389/fcvm.2021.636947
- Zou, Y., Li, S., Xu, B., Guo, H., Zhang, S., and Cai, Y. (2020). Inhibition of proprotein convertase subtilisin/kexin type 9 ameliorates liver fibrosis via mitigation of intestinal endotoxemia. *Inflammation* 43, 251–263. doi:10.1007/s10753-019-01114-x
- Zulkapli, R., Muid, S. A., Wang, S. M., and Nawawi, H. (2023). PCSK9 inhibitors reduce PCSK9 and early atherogenic biomarkers in stimulated human coronary artery endothelial cells. *Int. J. Mol. Sci.* 24, 5098. doi:10.3390/ijms24065098